

Polyphosphate Nanoparticles: Balancing Energy Requirements in Tissue Regeneration Processes

Werner E.G. Müller,* Meik Neufurth, Shunfeng Wang, Heinz C. Schröder, and Xiaohong Wang*

Nanoparticles of a particular, evolutionarily old inorganic polymer found across the biological kingdoms have attracted increasing interest in recent years not only because of their crucial role in metabolism but also their potential medical applicability: it is inorganic polyphosphate (polyP). This ubiquitous linear polymer is composed of 10–1000 phosphate residues linked by high-energy anhydride bonds. PolyP causes induction of gene activity, provides phosphate for bone mineralization, and serves as an energy supplier through enzymatic cleavage of its acid anhydride bonds and subsequent ATP formation. The biomedical breakthrough of polyP came with the development of a successful fabrication process, in depot form, as Ca- or Mg-polyP nanoparticles, or as the directly effective polymer, as soluble Na-polyP, for regenerative repair and healing processes, especially in tissue areas with insufficient blood supply. Physiologically, the platelets are the main vehicles for polyP nanoparticles in the circulating blood. To be biomedically active, these particles undergo coacervation. This review provides an overview of the properties of polyP and polyP nanoparticles for applications in the regeneration and repair of bone, cartilage, and skin. In addition to studies on animal models, the first successful proof-of-concept studies on humans for the healing of chronic wounds are outlined.

1. Introduction

Polyphosphate (polyP) is an ancient polymer that is found from prokaryotes to eukaryotes to metazoan animals.^[1–3] This physiological linear polymer is composed of hundreds of phosphate residues linked together by high-energy anhydride linkages (reviewed in: refs. [4–7]). Soon after the discovery of ATP^[8] and pyrophosphate,^[9] polyP was identified first as RNA^[10] and later as

W. E. Müller, M. Neufurth, S. Wang, H. C. Schröder, X. Wang
ERC Advanced Investigator Grant Research Group at the Institute for
Physiological Chemistry
University Medical Center of the Johannes Gutenberg University
Duesbergweg 6, D-55128 Mainz, Germany
E-mail: wmueller@uni-mainz.de; wang013@uni-mainz.de

 The ORCID identification number(s) for the author(s) of this article can be found under <https://doi.org/10.1002/smll.202309528>

© 2024 The Authors. Small published by Wiley-VCH GmbH. This is an open access article under the terms of the [Creative Commons Attribution License](#), which permits use, distribution and reproduction in any medium, provided the original work is properly cited.

DOI: 10.1002/smll.202309528

polyP^[11] with its energy-rich phosphate units.^[12] The initial studies on polyP were carried out in yeast.^[13] Three properties qualify polyP as an essential component of living cells; first, it is the element phosphorus that is indispensable for life, and second, this polymer allows self-replicating and enzyme-containing primordial living units to be compartmentalized as a coacervate,^[3,14,15] and third, it is an energy generator both in bacterial cells^[16] and the extracellular space of metazoans.^[17]

The interest in polyP, especially with regard to its application in human therapy, was pushed by the discovery that this polymer has an anabolic effect on biomineralization in bone and teeth.^[18–20] The importance of polyP for biomineral formation is understandable since ≈15% by weight of the human body consists of bone, a calcium phosphate (Ca-phosphate) mineral. Almost simultaneously it was shown, initially using spicules from sponges as an animal model, that not only organic materials but also inorganic materials (biominerals) in living organisms are formed enzymatically,

in sponges with the enzyme silicatein.^[21–23] Later, with the alkaline phosphatase (ALP) in mammalian bone,^[20,24] a further push toward the application of polyP for potential treatment in humans occurred. ALP is a polyP hydrolyzing enzyme.^[19] Since any kind of anabolic regeneration requires metabolic energy,^[25] with ATP being the main energy-carrying metabolite,^[26] it was reasonable to elucidate whether cleavage of the energy-rich bonds in polyP could be exploited for the generation of ATP. In fact, as described in this review, the transfer of energy from polyP to ATP was subsequently demonstrated experimentally.^[17] Thereafter, it was possible to successfully conduct proof-of-concept studies with polyP for the treatment of epithelia^[27] and chronic wounds.^[28]

2. Physiological Synthesis of polyP

In humans and other mammalian organisms, polyP is encapsulated in the dense granules of the blood platelets, which contain large amounts of ADP and ATP together with pyrophosphate and polyP.^[29,30] Platelets are abundant cell fragments in the blood that arise from megakaryocytes. When they are activated, polyP

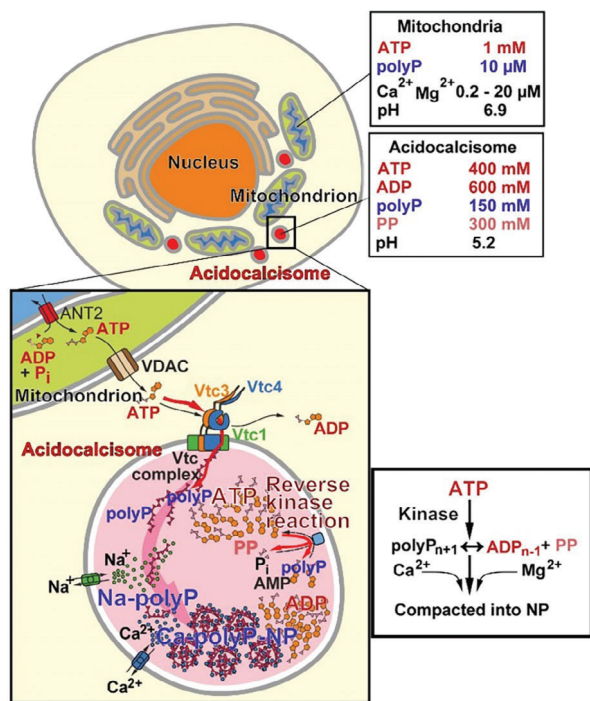


Figure 2. Proposed route of mammalian polyP synthesis. In mitochondria, the reduced coenzymes undergo oxidation in the respiratory chain, resulting in ATP synthesis. ATP is released from the matrix into the intermembrane space via the adenine nucleotide translocase 2 (ANT2) transporter and from there into the extra-mitochondrial cytosol via the voltage-dependent anion channel (VDAC). ATP accumulates in the adjacent dense granules, which correspond to the yeast acidocalcisomes with their Vtc complex, and might drive the synthesis of polyP by a postulated kinase, through a reversible reaction. Through dynamic exchange processes, the polymer forms either the soluble Na⁺ salt or Ca-polyP nanoparticles (Ca-polyP-NP). Subsequently, Ca-polyP-NP and Na-polyP are released into the extracellular space upon platelet activation.

removed from the reaction as it precipitates in the presence of divalent cations. Consequently, the overall reaction/equilibrium is shifted toward the polyP product (Figure 2).

In the dense granules and acidocalcisomes, which are rich in calcium, polyP is deposited as an electron-dense material. In this state, with Ca²⁺, the insoluble polyP most likely accumulates in the form of dynamic assemblies.^[48] The Ca-polyP deposits are assumed to undergo dynamic exchange with free polyP and most likely with other cations such as Na⁺. This dynamic deposition of polyP would also explain the finding that the polyP is released from these organelles as both insoluble Ca-polyphosphate nanoparticles (Ca-polyP-NP) and soluble Na-polyP.^[46]

2.2. The Two Phases of polyP: Soluble (Coacervate) and Particle-Associated Forms (Nanoparticles)

In the circulating human blood or in the blood plasma, polyP exists as soluble Na-polyP at a concentration of $\approx 1 \mu\text{g mL}^{-1}$ ^[33] or in a particulate/nanoparticle (NP) form.^[46] The polyP chains extruded from the platelets have a length of 60–100 P_i residues, while the NP-associated polyP is composed of longer polymers.^[46]

2.2.1. PolyP Chains in the polyP Coacervate

In the physiological environment, the polyanion polyP remains soluble only with Na⁺ as the counterion. The concentration of this cation in serum is $\approx 100 \text{ mM}$ (2.3 g L^{-1}), in contrast to Ca²⁺ at $\approx 2.5 \text{ mM}$ (90 mg L^{-1}). Under these concentration conditions, polyP remains in the soluble form but retains its chelating properties. It should be noted that Na⁺ is a harder cation and binds more strongly to hard counter-anions compared to Ca²⁺.^[49] At a concentration of $>5 \text{ mM}$ polyP (based on P_i), the polymer undergoes coacervation or NP formation, pH-dependently.^[50]

PolyP exhibits a biologically distinctive property, the formation of a coacervate. Coacervation is a process in which phase separation occurs, in the case of polyP during salt bridge formation between the polymer and smaller divalent metal cations such as Ca²⁺ or Mg²⁺. During the coacervation of polyP at pH 7, a Ca²⁺ shell is formed around the condensed polyP polymer phase.^[51] Based on modeling/simulation studies, binding of the monovalent cation Na⁺ to the polyP polyanion occurs in alternating order, while divalent cations (Ca²⁺ and Mg²⁺) bind to the polyP strand along an ordered peripheral line.^[52,53] **Figure 3-I.** Molecular dynamics simulations of the interaction of polyP and Ca²⁺ ions revealed that, at pH 7, both components first organize rather randomly, while in the following both partners sort themselves apart (Figure 3-IIA,B) and finally form two “layers” with polyP on one side and Ca²⁺ on the other side (Figure 3-IIC,D). These aggregates form liquid droplets, which further associated to organized, two-liquid-phase droplets in the aqueous environment. At pH 10, the Ca²⁺ and polyP components form concentric rings that condense to concrete particles, which further grow to NP that are (almost) devoid of water.^[52]

Coacervate assemblies are formed from a colloidal system via separation into two liquid phases. The material formed from polyP and Ca²⁺ ions is highly viscous (Figure 4-IA–C). At low magnification, the coacervate blocks appear with a compact morphology traversed by open cavities (Figure 4-ID). At higher magnification, it becomes overt that the coacervate blocks are interspersed with $\approx 30 \text{ nm}$ large granules embedded in the coacervate (Figure 4-IE). These granules are rarely suspended but predominantly associated with clusters via the aqueous gel (Figure 4-IF).

Compared to Ca-polyP-NP formation, the process of coacervation (Ca-polyP-Coa formation) at pH 7 is a slower process;^[52] Figure 4-IIA,B. Starting with a solution of 1.2 M CaCl₂ added dropwise to a 0.48 M Na-polyP solution with stirring (Figure 4-IIA), the reaction mixture becomes turbid and at a molar ratio of 1:2 (Na-polyP:CaCl₂) a viscous gel with a consistency of 10–15 cP^[53] is formed (Figure 4-IB,C).

FTIR spectra showed distinct differences between the Ca-polyP-Coa and Ca-polyP-NP as well as to Na-polyP and Ca-dihydrogen phosphate (Ca-P_i). According to published data,^[54–56] all polyP samples show the characteristic signals for $\nu_{\text{as}}(\text{P}=\text{O}-\text{P})$ at wavenumbers $\approx 863 \text{ cm}^{-1}$ and for $\nu_{\text{s}}(\text{P}-\text{O}-\text{P})$ at $\approx 733 \text{ cm}^{-1}$.^[52] In contrast, Ca-dihydrogen phosphate is distinguished by the presence of the signal $\nu_3(\text{PO}_3)^{2-}$ at 1021 cm^{-1} and for $\nu_4(\text{PO}_4)$ at 580 cm^{-1} . The Ca-polyP-NP comprises a distinct signal at a wavenumber of $\approx 1084 \text{ cm}^{-1}$ reflecting $\nu_{\text{as}}(\text{PO}_3)^{2-}$, a band that is only minor in the coacervate or the Na-polyP sample.

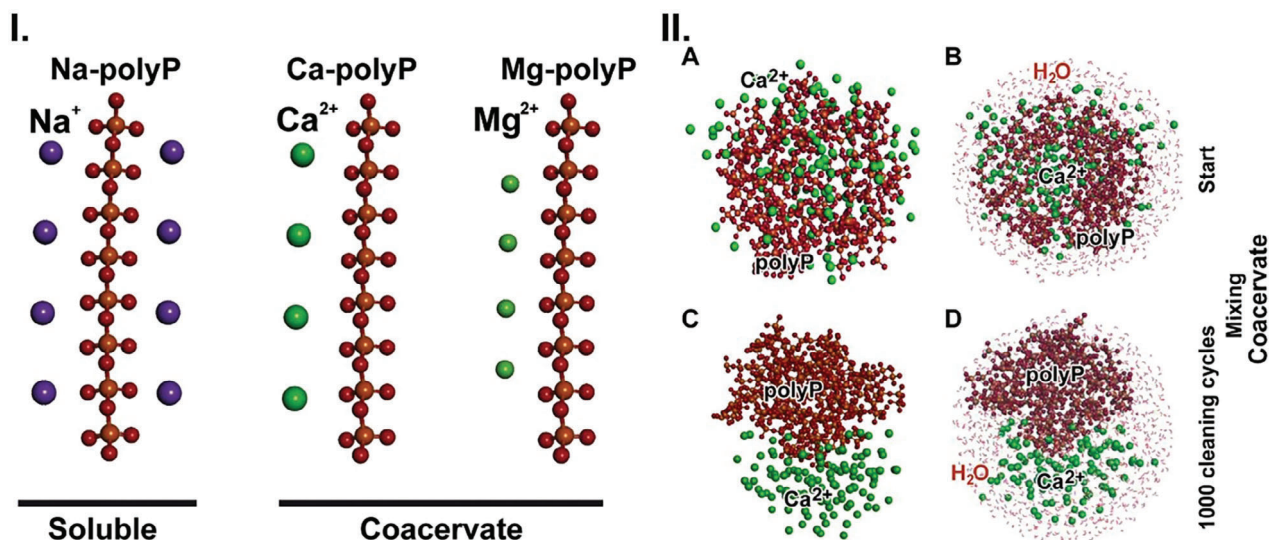


Figure 3. Coacervate formation at pH 7 and NP formation at pH 10. Molecular dynamics simulations. I) Structure of the polyP salts with monovalent and divalent cations. The simulation studies showed that the monovalent ions (Na⁺) are arranged alternately, while the divalent cations (Ca²⁺ and Mg²⁺) are located only on one side of the polyP strand. II) (A,B) At pH 7, the two components, polyP, and Ca²⁺, arrange stochastically and, after 1000 cleaning cycles, separate into a polyP cluster and a Ca²⁺ assembly. Then, in the aqueous phase, a liquid–liquid phase separation takes place under the formation of the coacervate. Reproduced with permission.^[53] Copyright 2023, Springer Nature Switzerland AG.

2.2.2. PolyP Transition from Coacervate to NP

Scanning electron microscopy (SEM) analyses of the samples from the turbidity studies (Figure 4-II) revealed that at pH 7 the coacervate phase is formed from Na-polyP and CaCl₂, while at pH 10 NP are assembled (Figure 5). The coacervate shows a block-like morphology at low SEM magnification (Figure 5A–C), while at higher magnification grain-like particles become visible (Figure 5D). At the beginning of the pH 10 titration phase, the collected particles, the grains, show an already rounded, NP-like morphology and are often decorated with particles, resulting in wrinkled surfaces. When the concentration ratio in the reaction

fluid reaches 480 mM CaCl₂ to 400 mM polyP, distinct rounded particles, termed NP, are formed (Figure 5E,F). The ultimately formed NP have a size of ≈100 nm (Figure 5G,H); they have a porous internal morphology (Figure 5H). From these data, it can be concluded that those NP are formed by assembly from the ≈30 nm-sized granules in the coacervate phase.

2.2.3. Growth of polyP Nanoparticles

In the presence of Ca²⁺, the phosphate anions are less soluble.^[57] The degree of solubility is dependent on the pH of the reaction

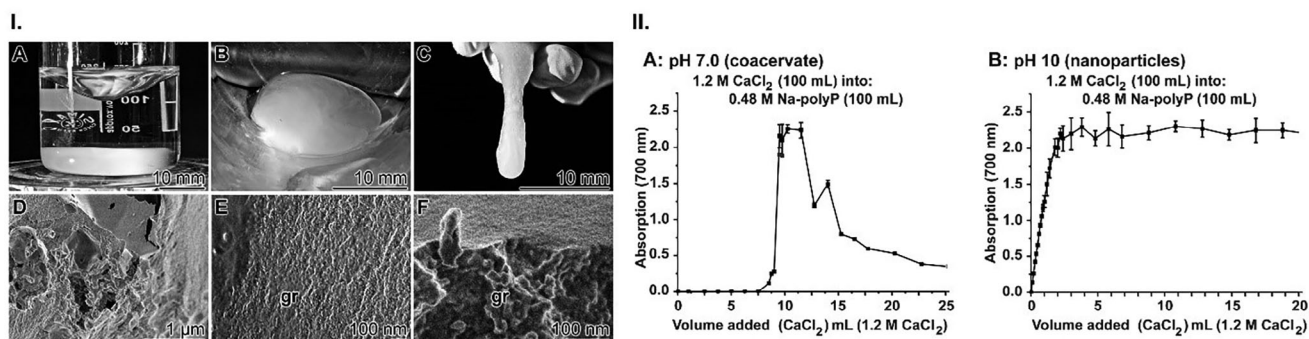


Figure 4. Coacervate formation and characterization. I) Coacervate formation from CaCl₂ and Na-polyP. Optically visible aggregate formation at pH 7.0. A) A CaCl₂ solution (14 g of CaCl₂•2H₂O in 100 mL) is added to a Na-polyP solution (5 g in 100 mL) at room temperature under vigorous stirring. After completion of the process, the B) coacervate with a C) viscous consistency is obtained. At low SEM magnification, D) the coacervate shows a solid morphology interrupted by open cavities. E,F) At higher magnifications, small (≈30 nm) granules (gr) embedded in the viscous coacervate appear. Reproduced with permission (Creative Commons Attribution License).^[14] Copyright 2018, WILEY-VCH Verlag GmbH & Co. KGaA, Weinheim. II) Optically visible aggregate formation from CaCl₂ and Na-polyP. In a volume-controlled setup, the appearance of aggregates either at (A) pH 7.0 or (B) pH 10 is monitored. At a pH of 7, the first aggregates appear later (after 6 mL) compared to the assay run at pH 10 (0.5–1.5 mL). Reproduced under the terms of the CC-BY-NC license.^[52] Copyright 2022, Elsevier Ltd.

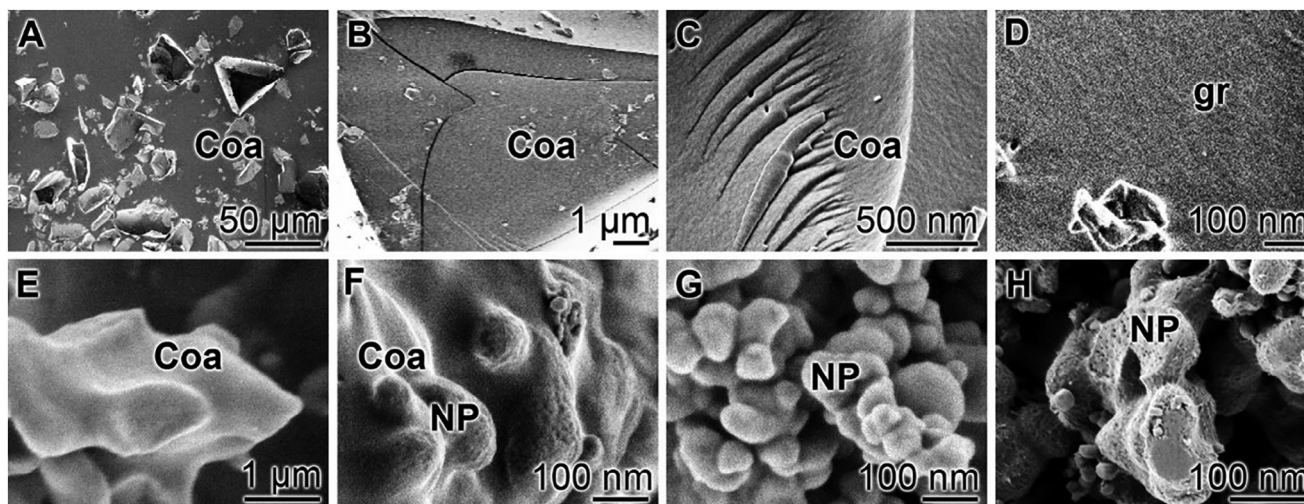


Figure 5. The transition from coacervate to NP. A–D) The coacervate (Coa) phase is formed at pH 7. A–C) At lower SEM magnification, the coacervate aggregates appear as blocks. D) At a higher magnification ≈ 30 nm grains (gr) appear within the liquid phase. E, F) After raising the pH to 10 the aqueous polymer coacervate droplets develop to NP. G, H) The NP has a porous internal morphology. A–D) Reproduced with permission (Creative Commons Attribution License).^[14] Copyright 2018, WILEY-VCH Verlag GmbH & Co. KGaA, Weinheim. E–H) Reproduced under the terms of the CC-BY-NC license.^[52] Copyright 2022, Elsevier Ltd.

mixture. Phosphoric acid is a weak triprotic Brønsted–Lowry base. Therefore, the concentration of its different dissociated forms, and hence the concentration of the soluble phosphorus, depends on the pH of the solution. The reactivity of PO_4^{3-} to free HPO_4^{2-} and H_2PO_4^- increases with decreasing pH. This means that with increasing pH (increase in PO_4^{3-}) the amount of insoluble Ca-polyP increases. The dissociation process is reversible, the equilibrium between the soluble metal cations and phosphate anions will be almost entirely on the side of the (almost) insoluble Ca-phosphate at pH 10.^[58] This chemistry could explain the growth of the particles/NP. Furthermore, the reversible conversion of NP to coacervate could also be formulated in this sense, which is needed for understanding the transformation of NP to the biomedically active coacervate form.^[14,56]

In the cells, polyP is stored in the dense granules or acidocalcisomes, organelles with a size ≈ 100 nm.^[42] Due to the Ca^{2+} environment, it can be assumed that polyP exists there as NP. It was a challenge to fabricate chemically Ca-polyP-NP of this size (≈ 100 nm) in order to assess their biomedical potential. Applying a superstoichiometric concentration ratio between soluble CaCl_2 and Na-polyP of 2:1, NP could be reliably prepared in an amorphous state at pH 10.^[59] Only in the amorphous form can these particles elicit biological activity.^[60] The biological activity of the NP is achieved via transformation into the coacervate phase of polyP.

2.3. Biological Importance of Cations in polyP Nanoparticles

The biomedical application of polyP is decisively dependent on the choice of the respective cation that forms the salt with polyP.^[61] This circumstance is closely related with the ion environment at the site where the polymer is formed and applied. As an example, the levels of Ca^{2+} (extracellularly normally ≈ 2.3 mM)

and Mg^{2+} (≈ 0.9 mM) show considerable fluctuations during regeneration, e.g., during wound healing. The Ca^{2+} level drops by 40% immediately after wounding, while conversely the Mg^{2+} concentration increases by 45%.^[62] This change is physiologically significant because Mg^{2+} stimulates cell migration into the injured region. In the later phase of cell proliferation, the concentration ratio between the two cations returns to the plasma levels. Ca^{2+} stimulates cell proliferation.^[63] This observation indicates that, in addition to the regeneratively acting polymer polyP, the respective cation in the wound bed is critical for the effectivity of the given polyP salt. Consequently, the choice of the counter-cation of polyP allows also a (possible) substitution of the ion milieu in the regeneration area.

PolyP is also suitable for application as Na-polyP, but with the potential adverse side effect that the polymer chelates divalent cations out and reduces thereby their bioavailability. As a smart biomaterial, polyP can guide divalent, substituting ions to the target site along with their own beneficial properties. Monocalcium phosphate (Ca-P_1) and Ca^{2+} tripolyphosphate (Ca-polyP_3) have crystal structures and morphologies in the anhydrous phase (Figure 6A,B,E,F).^[64–66] In solution, Na-polyP can immediately elicit its pharmacological activities, such as the generation of metabolic energy. In the presence of divalent cations, polyP forms NP at a superstoichiometric ratio and under alkaline conditions.^[59] Mg^{2+} accelerates the adhesion of mesenchymal stem cells to the fibrillar structures in the cartilage through conformational changes of the integrins and thereby promotes cartilage synthesis.^[67] The NP formed with this ion has a size of ≈ 500 nm (Figure 6C,D). Phosphate (PO_4^{3-}) is a hard base and tends to bind to hard acids such as Mg^{2+} . Ca^{2+} is less hard, larger than Mg^{2+} and has a lower charge state (the charge criterion applies mainly to acids, to a lesser extent to bases), and is weakly polarizable. With this cation, polyP of a chain length of 40 P_i units forms a smaller NP with an average diameter of ≈ 150 nm (Figure 6I,J). Down the hardness scale, Sr^{2+} -polyP particles are

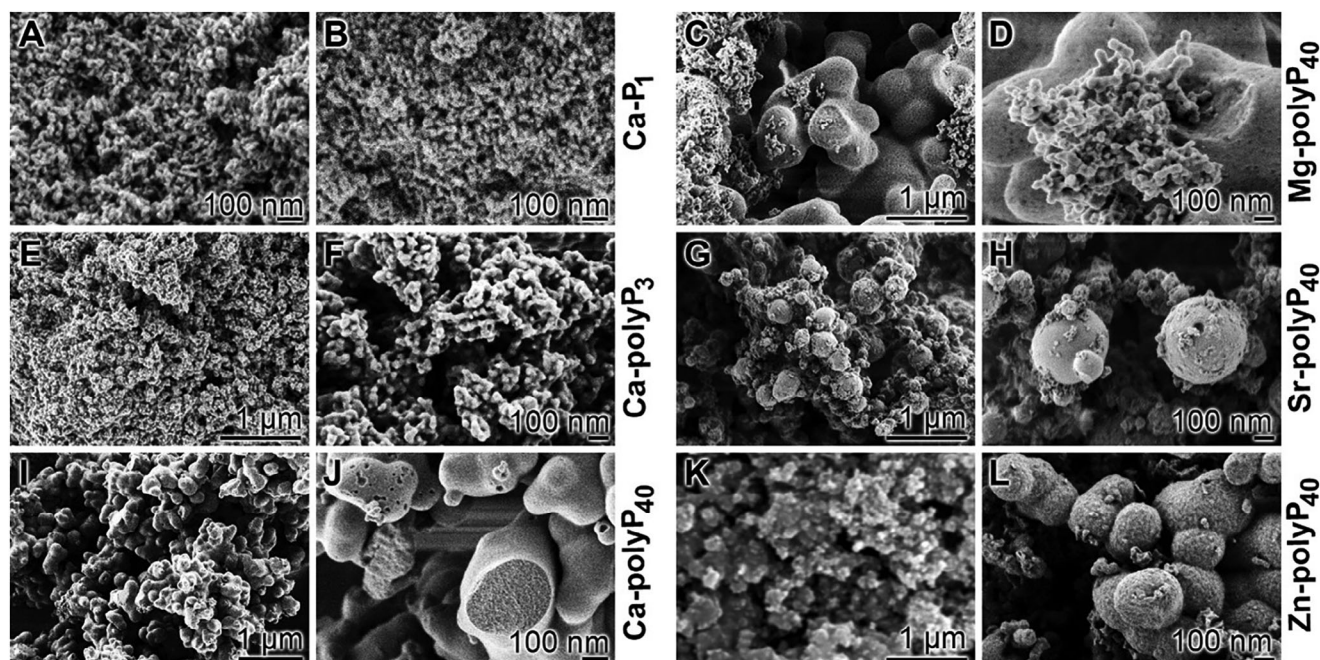


Figure 6. Morphology of therapeutically important phosphate/polyP particles formed with divalent ions; SEM analyses. A,B) Monocalcium phosphate (Ca-P₁); E,F) Ca²⁺ tripolyphosphate (Ca-polyP₃), and I,J) Ca²⁺ polyP with a chain length of 40 P_i units (Ca-polyP₄₀). Then, C,D) NP are shown that are prepared from Na-polyP with 40 P_i units and Mg²⁺ as the cation (Mg-polyP₄₀), or G,H) Sr²⁺ (Sr-polyP₄₀), as well as of K,L) Zn²⁺ (Zn-polyP₄₀). A–H) Reproduced with permission.^[61] Copyright 2018, The Royal Society of Chemistry. K,L) Reproduced with permission.^[64] Copyright 2020, The Royal Society of Chemistry.

similarly sized (Figure 6G,H) and for Zn²⁺ NP an average size of ≈150 nm was determined (Figure 6K,L).

Sr²⁺, as an alkali-earth metal cation, was found to increase the synthesis activity of osteoblasts and is present in higher amounts in the metabolically active trabecular bone compared to cortical bone.^[68] In addition, polyP in the form of Zn-polyP NP supports the growth and migration of epidermal keratinocytes, which also makes this formulation a candidate for wound regeneration.^[64]

2.4. Interaction with Proteins

Recent studies have shown that polyP may have an additional role in regulating protein activity: PolyP exhibits a chaperone-like activity.^[69] The polymer is able to protect cells from stress-induced protein aggregation.^[69,70] PolyP binds and stabilizes misfolded proteins in a soluble β -sheet-rich conformation, thereby preventing their aggregation.^[70] This mechanism (based on the stabilization of β -sheet-rich unfolding intermediates) is thought to be involved in the protective effect of polyP on neuronal cells against the toxicity of amyloidogenic proteins such as Alzheimer's A β protein and may therefore be of interest in diseases that are associated with the deposition of amyloid fibrils.^[69,71] In addition to its effect on amyloid aggregation in neuronal tissue, the chaperoning activity of polyP also appears to be involved in the antiviral, anti-SARS-CoV-2 activity of the polymer.^[27,72] PolyP has been reported to interact specifically with the receptor binding domain of the viral spike protein,^[27] preventing receptor binding and cell infection, but also intracellularly with the host receptor protein angiotensin-converting en-

zyme 2 (ACE2) as well as the SARS-CoV-2 RNA-dependent RNA polymerase (RdRp).^[72] The binding of polyP to positively charged amino acids of the latter proteins leads to their enhanced proteasomal degradation, resulting in inhibition of SARS-CoV-2 replication, as both demonstrated in various cell lines infected with the virus and in experiments with primary human nasal epithelial cells exposed to nebulized SARS-CoV-2.^[72] This effect could be suppressed by adding the proteasome inhibitor MG-132.

2.5. Distribution of polyP in Eukaryotic Cells and Tissue

In the precursor cells of the platelets, the megakaryocytes, ATP is generated in the mitochondria during the enzyme/coenzyme-driven respiratory chain. Glucose is metabolized to lactate/pyruvate and transported into the mitochondrial matrix where it is oxidatively decarboxylated to acetyl-CoA. In the citric acid cycle, the reduced coenzymes NADH and FADH₂ are formed. These coenzymes then undergo reoxidation to NAD⁺ and FAD, which is coupled with ATP production via mitochondrial ATP synthase. ATP crosses the inner mitochondrial membrane through the adenine nucleotide translocase (ANT2) and from there the outer mitochondrial membrane through the voltage-dependent ion channel (VDAC) and reaches the cytoplasm; Figure 2. We propose, as mentioned above, that within the dense granules/acidocalcisomes, Ca²⁺-bound polyP is synthesized from the abundantly present ATP via the postulated (reversible) kinase(s) reaction(s); Figure 2.

It is essential that any nutrient, energy-delivering system, cytokine or growth factor required for regeneration reach the

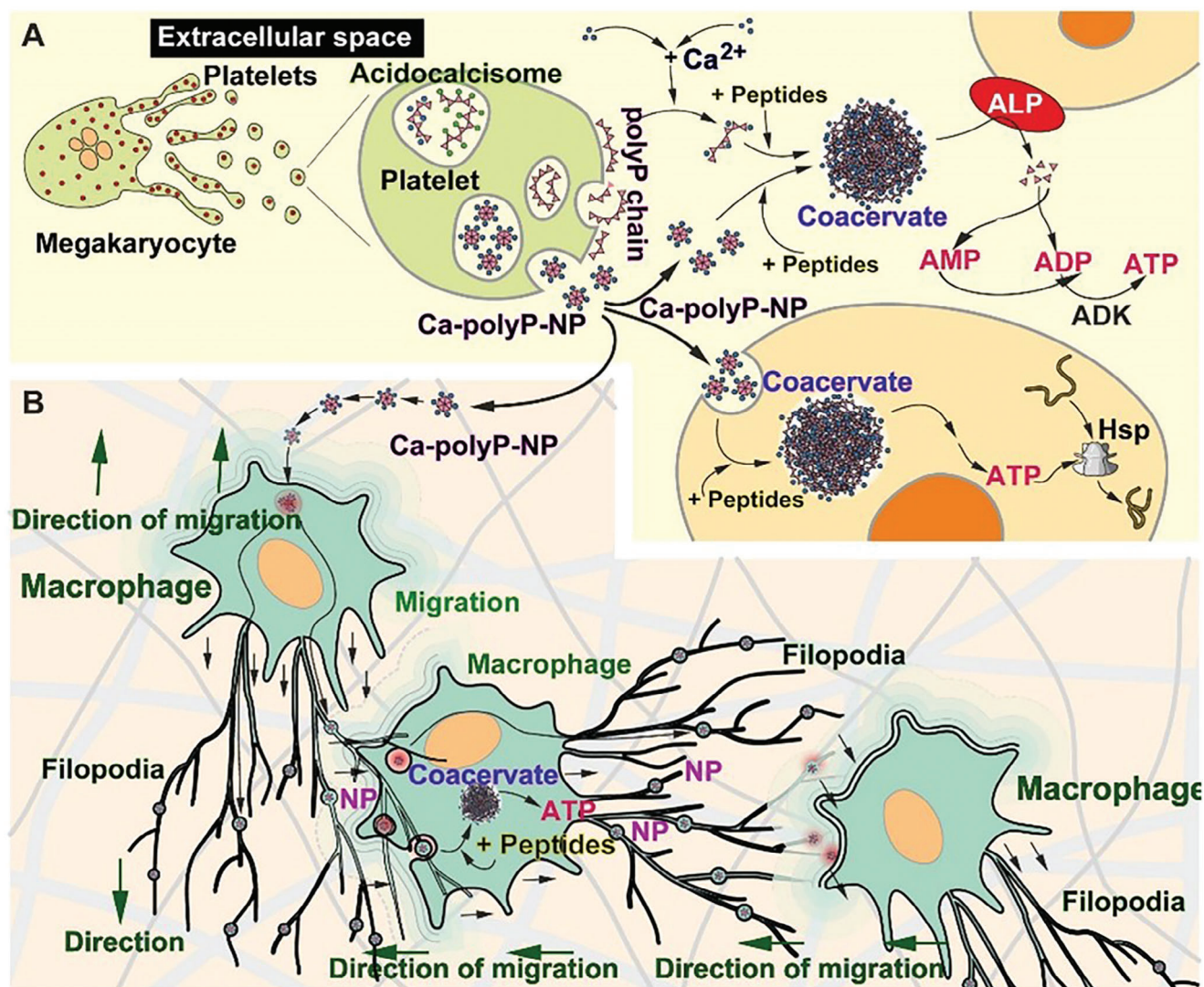


Figure 7. Proposed distribution pathways for Ca-polyP-NP. A) In the extracellular space, the platelets produced by megakaryocytes harbor the bulk of the polyP and primarily distribute polyP in the circulating blood. They release the two forms of polyP (Na-polyP and Ca-polyP-NP), which are subsequently enzymatically cleaved by ALP. The liberated free energy is stored in ADP, which is further processed to ATP in the presence of ADK (adenylate kinase). B) In addition, it is proposed that the macrophages, which readily engulf NP, are involved in supplying injured regions with polyP. These cells comprise migrasomes, organelles produced by migrating cells; they can be filled with NP. The migrasomes migrate along long, retracting fibers.

site of need in a fast equally safe, and economically potent manner. In this regard, the vascular system is most effective. This is particularly important for processes involved in repair of osteochondral defects affecting cartilage, cartilage-bone interface, and subchondral bone. Importantly, the vascularized periosteum contributes essentially to a successful blood supply.^[73] Even in the case of extensive wound regeneration, an operant restoration of the blood circulation must first take place.^[74] After reaching the damaged site to be repaired, the blood, which contains the required physical and chemical factors, such as oxygen, nutrients, and regulatory factors, can initiate cell proliferation and remodeling. Growth factors such as bone morphogenetic proteins^[75] are also formed together with the (compartmentalized) polyP in megakaryocytes, from which the platelets (thrombocytes) originate.^[76] These small

cell fragments play a key role in every type of tissue repair in mammals.

Upon platelet activation in response to tissue injury,^[77,78] polyP is released from the platelets in two forms, either in the soluble form, as polyP complexed with Na^+ cations, or as insoluble NP with Ca^{2+} , as Ca-polyP-NP with a size of $\approx 300 \text{ nm}$;^[46,79] **Figure 7A.** The polyP chains in the soluble polyP fraction released from the platelets are short with a polymer length of 60–100 P_i residues. In the acidocalcisomes and dense granules, both the pH milieu (5.4) and Ca^{2+} concentration (70 mM) are suitable for NP formation.^[80] The release of the two forms of polyP, soluble and nanoparticulate, from the platelets occurs in a controlled manner^[81,82] as proposed.^[46] In the circulating blood after full platelet activation, the concentration of polyP is relatively high with $0.5\text{--}3 \mu\text{g mL}^{-1}$.^[46,83] The level of Ca-polyP-NP has not yet

been determined due to analytical difficulties. PolyP in the circulating blood or plasma released from activated platelets has only a short half-life with $\approx 1.5\text{--}2\text{ h}$,^[84] compared to quiescent platelets with a life-span of 7–10 d; their density is high with $150\text{--}400 \bullet 10^3$ platelets per mL. The polyP molecules are of short to largely short chain lengths with $\approx 50\text{ P}_i$ units for Na-polyP and $\approx 150\text{ P}_i$ units for the particle-associated form when released from the platelets into the bloodstream. In the circulating blood, polyP, which is incorporated into NP, remains attached to the platelet surface while the soluble polymer chains are set free.^[79] When the platelets are exposed to the extracellular matrix (ECM), they are activated by interaction with collagen and laminin, and also with fibrinogen during vascular events.^[85] The activation of the platelets upon contact with ECM proteins occurs via their adhesion receptors, especially if the endothelial barrier is disrupted.^[86,87]

The concentration of Ca^{2+} in the serum is low at $80\text{--}100\text{ }\mu\text{g mL}^{-1}$ ($\approx 2.3\text{ mM}$),^[83] in contrast to Na^+ at 5.7 mg mL^{-1} (142 mM). In turn, the released Na-polyP undergoes at least partial coacervation. The second form of polyP released from platelets is Ca-polyP-NP. This formulation is particulate and, in turn, insoluble. The platelets are the principal disseminating cells in the circulation system. There, via the platelets, polyP is transferred to other body cells where the polyP undergoes enzymatic hydrolysis and processing, generating metabolic energy (ATP);^[17] Figure 7A.

Since polyP has a strong potency to regulate the metabolism and defense state in macrophages,^[88–90] one might assume that these cells, in addition to the platelets, act as vehicles for NP to be distributed in the body (Figure 7B). These migration-competent cells, which are important for the inflammatory status, produce migrasomes, which are loaded onto retraction fibers that trail behind these migrating cells, the podocytes.^[91] The migrasomes are vesicular structures filled with cellular contents and small vesicles. Platelets also produce migrasomes, which they release after activation.^[92] It is very likely that Ca-polyP-NP is also involved in this recently published cell migration pathway. The macrophages migrate both in the plasma and in the intercellular matrix as well as in the basement membrane along the fibronectin network.^[93] In this cell vehicle the components, polyP, are distributed throughout the body.

3. Distinguished Property of polyP: Generation of Metabolic Activity

Exposure of SaOS-2 cells to Ca-polyP-NP revealed a significant increase in the ATP level in the extracellular space (culture medium).^[94,95] The first distinct hint that polyP anabolically up-regulates the energy production of the cells came from TEM (transmission electron microscopy) analyses, which showed that cells grown in the presence of polyP have a high accumulation of mitochondria adjacent to the cell nucleus (Figure 8-ID–F), while normal numbers of these organelles are seen in controls (Figure 8IA,B).

The generation of ATP by polyP involves two enzymes, ALP and adenylate kinase (ADK).^[17] The ALP is a ubiquitous, often membrane-bound ecto-enzyme^[96] that hydrolyzes polyP from the ends of the polymer. This enzyme degrades polyP in a processive manner.^[97] The mechanism has been described in detail.^[17]

In response to polyP, cells, mostly SaOS-2 cells and mesenchymal stem cells (MSC) have been used, migrate directionally, and begin to organize into microvessels. This process can be abolished or significantly prevented by the addition of levamisole, an established inhibitor of ALP,^[98] as well as by the natural ADK inhibitor, $\text{P}^1, \text{P}^5\text{-di(adenosine-5')pentaphosphate}$.^[99] The inhibitor studies supported the conclusion that during the release of P_i from polyP, the generated metabolic energy is used for the synthesis of ADP from AMP. ADP is then up-phosphorylated by ADK to ATP.^[17,100] In turn, polyP acts as a reservoir for metabolic energy in eukaryotes and especially in the extracellular space of tissues in animals since the beginning of their development.^[16,101] The generation of ATP by SaOS-2 cells depends on the concentration of polyP, as shown here by exposing these cells to Ca-polyP-NP in the range between 3 and $30\text{ }\mu\text{g mL}^{-1}$ (Figure 8-II). Overall metabolic activation of the cells with the mineralization activation cocktail^[102] composed of β -glycerophosphate, ascorbic acid, and dexamethasone boosts ATP production considerably.

4. Current Areas of Application of the polyP NP

Basically, any area of the body that is injured is subject to polyP substitution and regeneration therapy with polyP.^[17] The delivery of polyP focuses primarily on those areas that are not sufficiently supplied with blood and thus with polyP via the blood platelets. At risk are patients suffering from thrombocytopenia, for example during sepsis,^[103] chronic wounds,^[104] bone fractures,^[105] and bone marrow disorders.^[106] The economic burden on society is high; just for example, the expenditures for chronic wounds in the US have been estimated at $\$28.1\text{--}\96.8 billion.^[107]

The fields of application of polyP-NP in human therapy have been elucidated in the last years, and even proof-of-concept studies have confirmed the substantial beneficial effect of polyP and its NPs. Here we focus on the effects of the polymer in the field of hard tissues (bone) and soft tissues (cartilage and wound healing); Figure 9.

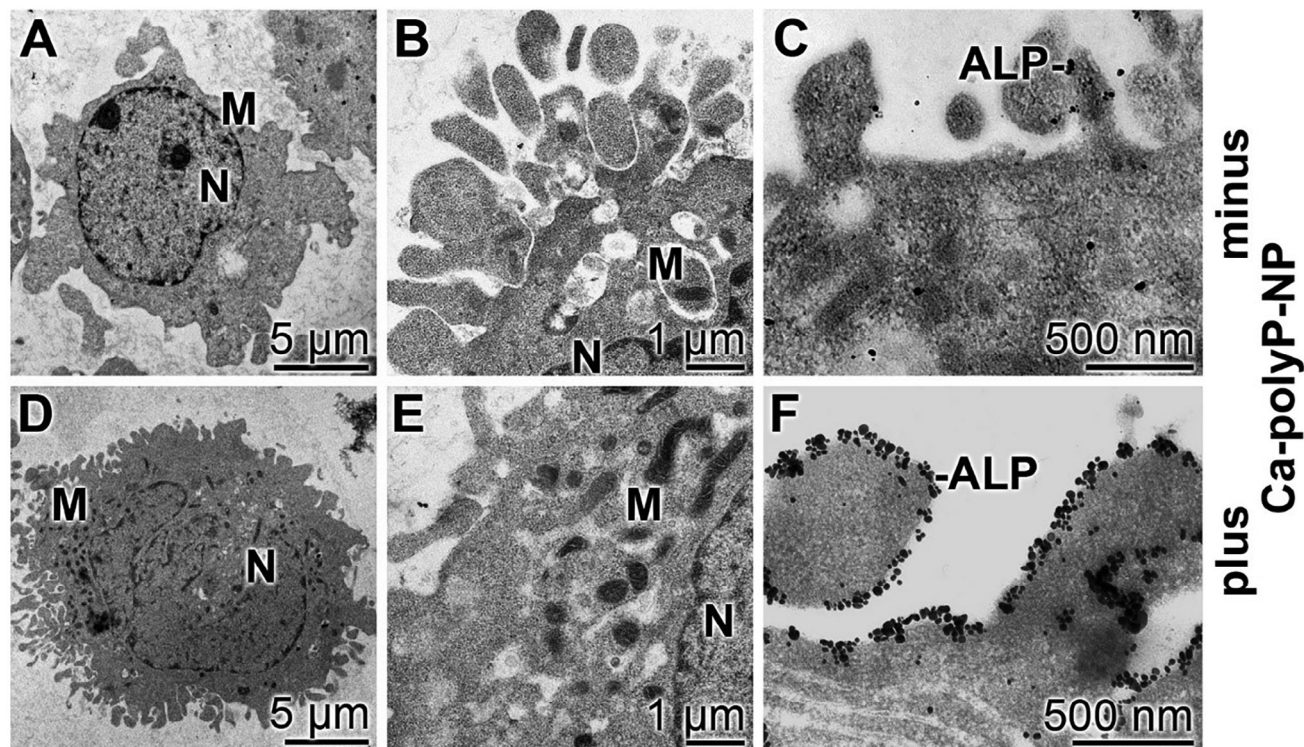
4.1. Bone Fracture Healing

Bone is built of organic fibers (such as collagen), 60–70% minerals Ca-phosphate components, and only $\approx 15\%$ water. The blood circulation is limited and bone is hypoxic in some regions, such as the diaphysis, which is devoid of any arterial blood supply. In contrast to this region, which is the midsection (shaft) of a long bone, the apical metaphysis portion with its cartilaginous component (epiphyseal plate) together with its fibrous component, the growth plate of the bone, is heavily vascularized and supplied with blood.

4.1.1. PolyP a Physiological Regulator of Bone Mineral Crystallization

It is established that the mineral deposits in the human body are first deposited as amorphous material that is biologically active and then processed to crystalline minerals.^[56] This holds true

I.



II.

Extracellular ATP generation

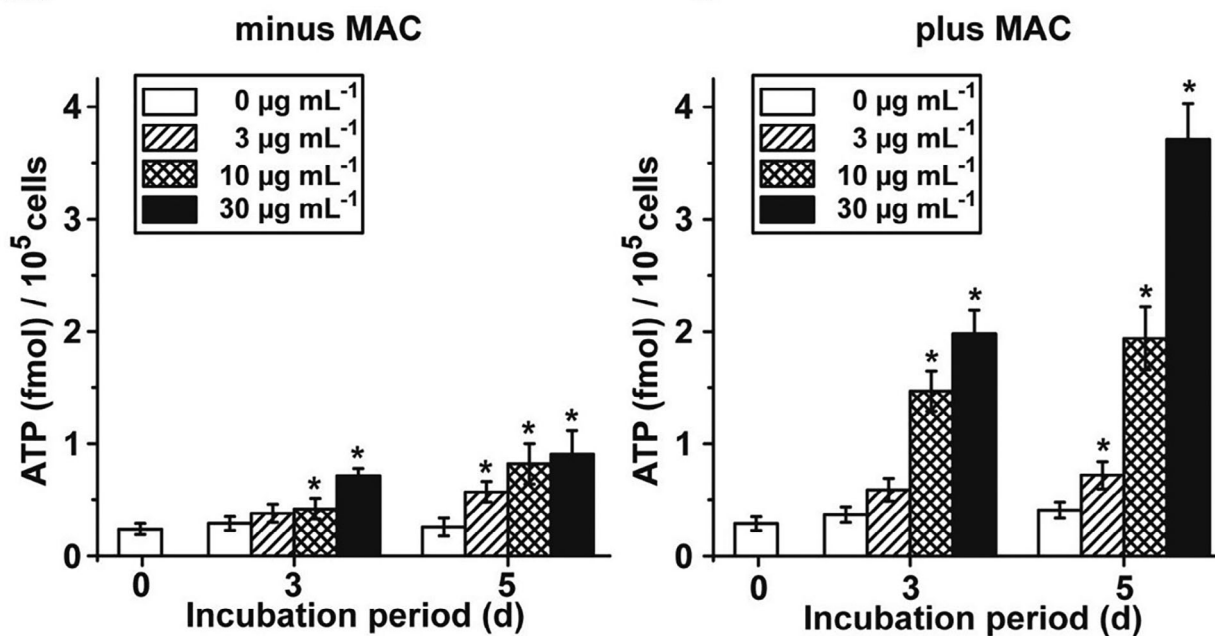


Figure 8. Generation of ATP in response to Ca-polyP-NP incubation in SaOS-2 cells. I) The cells were incubated either in the A–C) absence polyP or were D–F) exposed to $30 \mu\text{g mL}^{-1}$ of Ca-polyP-NP; TEM. In the absence of the polymer, the abundance of mitochondria (M) in the cells is low, while in the assays with the polymer, their density is high. The cell nucleus is also marked (N). By applying the immunogold labeling technique, the localization of the alkaline phosphatase (ALP) becomes visible; compared to the controls, the density of the ALP immune complexes on polyP-treated cells is high. II) The level of ATP in the extracellular space of SaOS-2 cells increases after exposure of the cells to 3, 10, and $30 \mu\text{g mL}^{-1}$ of Ca-polyP-NP significantly (*). After activation of the cell metabolism with the mineralization-activation cocktail (MAC) the level of ATP increases drastically. Reproduced under the terms of the CC-BY license.^[94] Copyright 2015, The Company of Biologists Ltd.

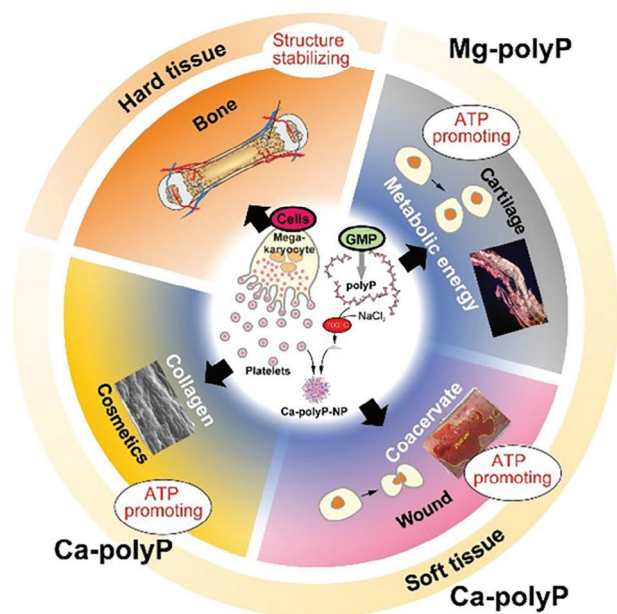


Figure 9. The major application routes of polyP in regenerative medicine, for the repair of hard tissue (bone) and soft tissue such as cartilage and in wound healing or cosmetics.

also for the mineral phase of bone, hydroxyapatite (HA). The non-crystalline precursor of HA is amorphous Ca-phosphate (ACP). This phase can be stabilized by polyP at a percentage of >15% by weight.^[108,109]

Central to HA formation is the enzyme ALP, more precisely a specific isoform, the tissue-nonspecific alkaline phosphatase (TNAP), which is strongly expressed in bone, liver, and kidney and plays a key role in the calcification process of bone.^[110] This enzyme not only hydrolyzes pyrophosphate, an inhibitor of biomineralization at least in vitro systems.^[111] It also provides inorganic phosphate (P_i), which is needed as a source for Ca-phosphate deposition in bone. Pyridoxal phosphate and β -glycerophosphate are considered organic sources of P_i .^[102] However, these precursors are quantitatively not sufficient to provide phosphate for HA formation in the body.^[112] Since the sites for initial bone formation are highly vascularized^[113] and the number of platelets increases during reshaping and reorganization during embryonic development,^[114] it is most likely that it is polyP that is the major P_i supplier for bone mineralization.^[112] This polymer, polyP, stabilizes the amorphous precursor of HA and it is the ALP that controls the kinetics of transformation of the precursor into the crystalline phase.^[109] This transition process of ACP to crystalline Ca-phosphate (CCP) and then to HA can be traced by FTIR (Figure 10A) and also by SEM (Figure 10B). The amorphous ACP state is characterized by a non-split $\nu_4(\text{PO}_4)$ vibration at a wavenumber of 580 cm^{-1} . Incubation of ACP with ALP (bovine intestinal mucosa) for 60 min, especially for 180 min, leads to a gradual splitting of this vibration signal^[109] into two distinct peaks at 599 and 557 cm^{-1} . This shift reflects the transformation from ACP to CCP.

In parallel, X-ray diffraction (XRD) analyses were performed (Figure 10C). The diffractograms show that ACP shows no signs of crystallinity at the beginning of the incubation with ALP, while

after 60 and 180 min incubation with the enzyme distinct and characteristic peaks at 30.2° , 46.6° and 54.8° are recorded that are characteristic for HA.^[115] SEM analyses confirmed that ACP has a globular shape, while CCP particles are angular to cubic (Figure 10B).

4.1.2. PolyP the Physiological Driving Force of Bone Formation

Two major components drive bone (HA) synthesis, first, phosphate (P_i), which processes fibrous tissue to HA, a crystalline Ca-phosphate ($\text{Ca}_{10}[\text{PO}_4]_6[\text{OH}]_2$), and, second, metabolic energy. The cells involved in bone formation, osteoblasts, and osteoclasts, are provided with sensitive energy-monitoring mechanisms such as the AMP-activated protein kinase and the mechanistic target of rapamycin (mTOR) pathway to control bioenergetics and ATP synthesis in cells of the osteogenic lineage.^[116] Furthermore, extracellular ATP is a decisive autocrine and paracrine signaling molecule for bone and muscle cells.^[117] Not only bone synthesis but also bone resorption is an energy-intensive metabolic process. An imbalance of both processes contributes to the development and progression of osteoporosis.^[118]

Both cornerstones required for bone formation, phosphate, and metabolic energy, are provided by polyP. First, phosphate: as mentioned, polyP is transported to the tissues, including bone, via the blood platelets. There, Na-polyP and also Ca-polyP-NP are subject to enzymatic hydrolysis. In the case of the Ca-polyP-NP, the particles must be enzymatically disintegrated. During this physical/chemical process, the particulate polyP becomes soluble in the coacervate phase. In this state, the polyP can be enzymatically hydrolyzed to P_i , which is then fed to the ACP precursor, most likely amorphous calcium carbonate (ACC), which is subsequently transformed to ACP in the presence of P_i (Figure 11).^[119]

Second, metabolic energy: during cleavage of the energy-rich phosphoanhydride bonds by ALP, the released Gibbs free energy is stored in AMP to ADP;^[17] Figure 7A and Figure 11. The generated ADP undergoes up-phosphorylation to ATP via ADK under the formation of ATP and AMP. ATP is required for phosphorylation of a central protein, the dentin matrix protein 1 (MP-1), present in the ECM of teeth and bone.^[120] Impaired expression of MP-1 leads to osteomalacia with hypo-mineralized tissues due to abnormal phosphate supply to the bone-forming centers.^[121] MP-1 modulates the transcription factor core-binding factor 1 (Cbfa1), which is a runt domain family member, and through this interlink, MP-1 is a key molecule in cartilage and bone development.^[122] The functional activity is controlled by the Fam20C kinase.^[123]

These two prerequisites for a metabolic synthesis and regeneration of bone are met by Ca-polyP-NP with the supply of P_i and metabolic energy; even Ca^{2+} is delivered via this route.

In its capability to provide metabolic energy (ATP) required for energy-dependent tissue regeneration, polyP fundamentally differs from other materials used for bone regeneration that are based on calcium phosphate. These materials such as β -tricalcium phosphate (β -TCP) or HA are widely used as bone substitute materials or bone fillers, and their osteoconductive and sometimes osteoinductive properties have been extensively studied.^[124] The regeneration activity of the latter materials is largely based on the release of calcium and phosphate ions,

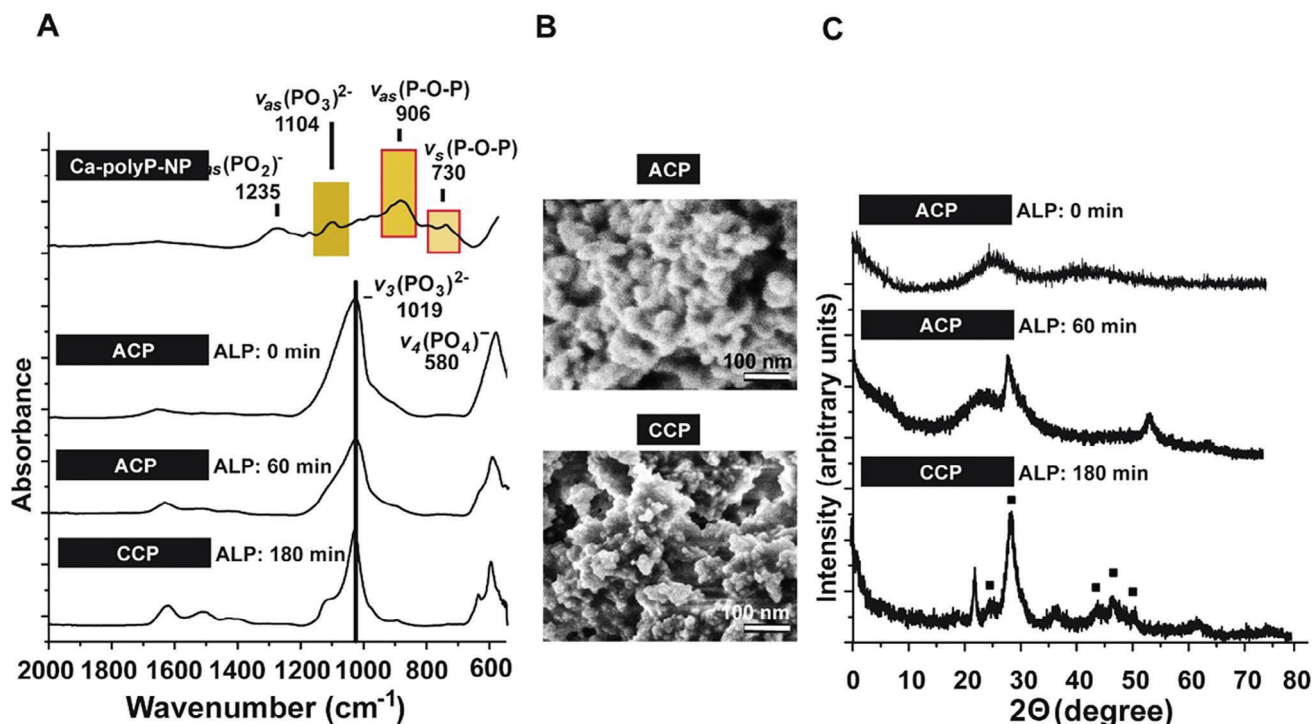


Figure 10. Effect of incubation with the enzyme ALP on the transition kinetics of ACP (amorphous Ca-phosphate) stabilized by 15% (by weight) of polyP to CCP (crystalline Ca-phosphate). A) The FTIR spectrum of ACP shows no splitting at the $\nu_4\text{PO}_4$ band, while a split pattern appears during incubation with ALP for 60–180 min. B) Morphology of ACP (globular shape; top) versus CCP (angular to cubic morphology; bottom). C) XRD spectrum of CCP with distinct crystalline signals (cube symbols); the diffractogram for the initial ACP state does not show a sharp peak. After 60 min of ALP treatment, the first sharper peaks appear. A) Reproduced with permission (Creative Commons Attribution).^[61] Copyright 2018, The Royal Society of Chemistry. B,C) Reproduced with permission.^[109] Copyright 2022 The Academy of Dental Materials. Published by Elsevier Inc.

which are involved in the regulation of maturation and function of osteoblasts and osteoclasts.^[125] They induce the expression of osteoblast differentiation marker proteins such as ALP, collagen type I, and bone morphogenetic proteins, are involved in signaling pathways (calcium), and provide the materials for

bone mineral deposition.^[124,126] However, these materials lack the metabolic energy (ATP) providing function shown by polyP.

There are only a few other strategies to stimulate tissue regeneration by enhancing energy production. However, in contrast to polyP, these strategies rely on the delivery of

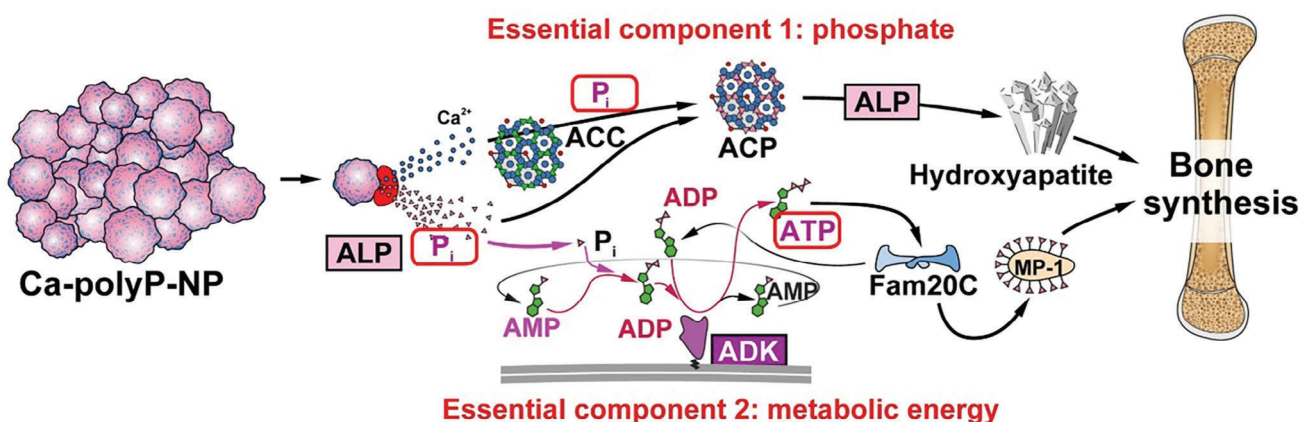


Figure 11. The two prerequisites for controlled synthesis and regeneration of bone; P_i and metabolic energy. Ca-polyP-NP is processed by ALP under the release of P_i . Phosphate is needed for the conversion of ACC to ACP, which proceeds in the absence of enzymes. From the amorphous state, Ca-phosphate (ACP) matures to hydroxyapatite after enzymatic hydrolysis of the polyP constituent. The release of Gibbs free energy that accumulates during hydrolysis of the energy-rich bonds in polyP is (partially) stored in ADP, which is subsequently converted to ATP. ATP, in turn, feeds the Fam20C kinase while phosphorylating the bone/dentin matrix protein 1 (MP-1). MP-1 is a major controlling factor in bone formation.

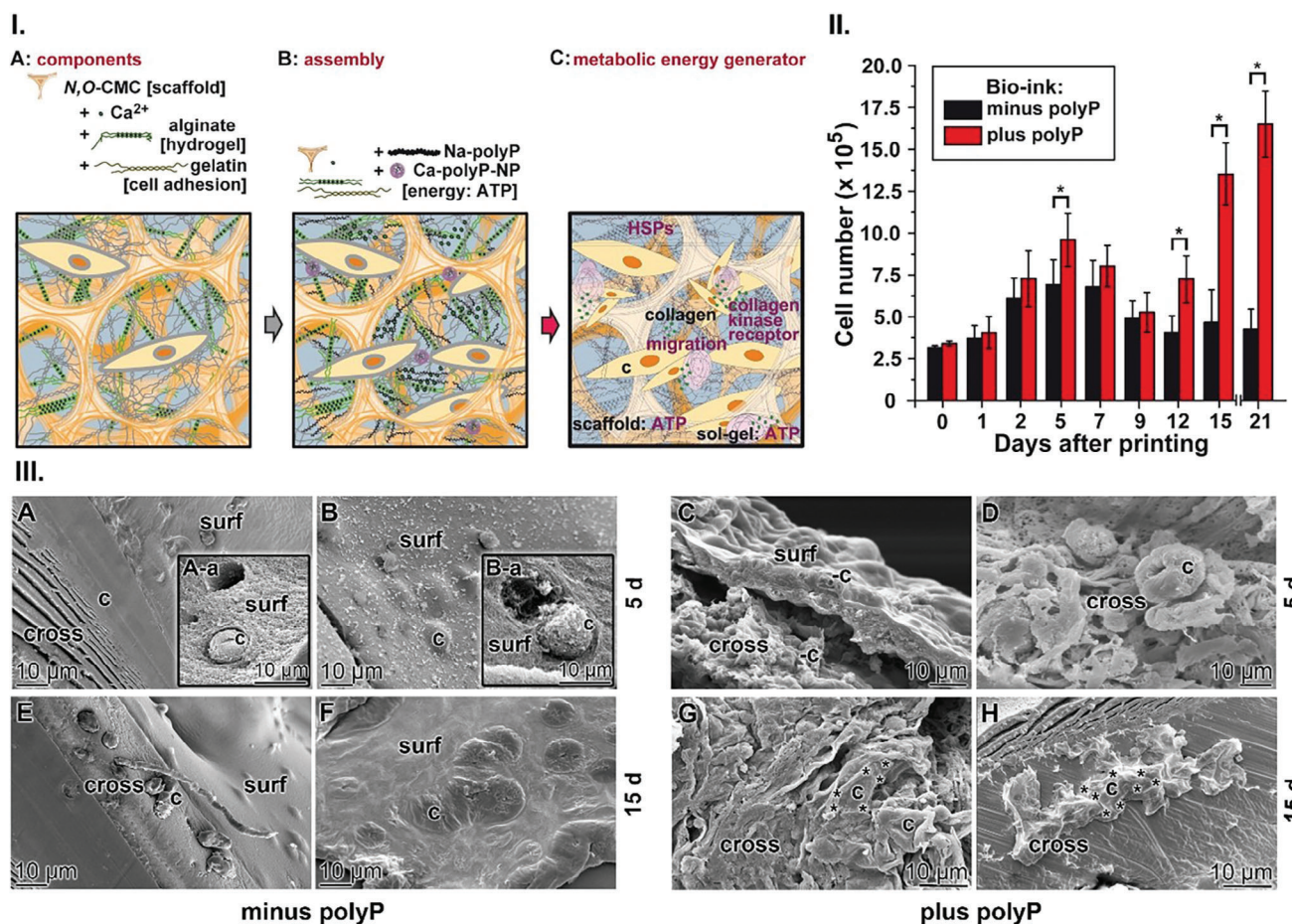


Figure 12. The 3D printing of a hydrogel supplemented with polyP. I) Hierarchical composition and organization of the innovative hydrogel. A) The components: *N,O*-CMC used for stabilizing the scaffold, alginate for the formation of the Ca²⁺ cross-linked hydrogel, gelatin for the provision of the adhesion substrate (R-G-D sequence) to the cells, and Ca-polyP-NP as a supply of metabolic energy. II) Kinetics of MSC growth in the bioink in the absence (minus) or presence (plus) of polyP. After the indicated incubation periods, the cell densities were determined colorimetrically. III) Growth of the MSC in the hydrogels in the (left panel [A, B, E, F]) absence (minus) or (right panel [C, D, G, H]) presence (plus) of polyP. The major differences in the growth pattern between the two hydrogels are the higher cell (c) density of the polyP hydrogel, the distribution pattern of the cells on the hydrogel surfaces (surf), and the arrangement of the cells. In the stratified cross fractures, it can be detected that in the presence of polyP the lobate cells (some boundaries are marked [*]) aggregate to clusters; SEM images. Reproduced under the terms of the CC BY 4.0 DEED license.^[129] Copyright 2021, The Author(s). Published by IOP Publishing Ltd.

intracellular (not extracellular) ATP, either through the application of ATP-containing vesicles^[127] or through a bioenergetically active, poly(glycerol succinate)/ethanediol-based material that increases mitochondrial energy production. This material is gradually degraded into fragments that are internalized to increase the mitochondrial membrane potential and accelerate bone regeneration.^[128]

4.1.3. 3D Bioprinting of Tissue Units

PolyP has also been successfully used for the formulation of a bioink suitable for 3D bioprinting with cells.^[129] The bioink was composed of *N,O*-carboxymethyl chitosan (*N,O*-CMC; as a structural component), alginate (the hydrogel) and gelatin (cell adhesion matrix), and polyP as the metabolic energy-providing component (Figure 12-IA-C). The components were hierarchi-

cally composed and organized in the bioink. As a basic scaffold *N,O*-CMC was chosen to provide stability (Figure 12-IA). Then, alginate was added, which was thereupon bathed in Ca²⁺ solution to form a hydrogel. In addition, the material was supplemented with gelatin to provide the adhesion substrate to the cells (Figure 12-IA). Finally, Ca-polyP-NP was supplemented to enrich the hydrogel with the source of metabolic energy (Figure 12-IB).^[129] ATP, generated, served as fuel for heat shock proteins or kinases such as extracellular protein tyrosine kinases.^[130] It was found that, in this hydrogel, the cells (MSC) readily proliferate especially within their cavities.^[129] A biphasic growth kinetics was determined with a first peak after 5 days (increase of the cell density from 2.5×10^5 to 9.7×10^5 cells mL⁻¹) and a second one after 15 days (to 17.1×10^5 cells mL⁻¹) (Figure 12-II). It is very remarkable that the proliferation potency continued further to 21 days. This strong proliferation was found only in the hydrogel enriched with polyP; in the hydrogel without

polyP, the growth/proliferation capacity of the cells was significantly lower.

The distribution and density pattern of the MSC within the bioink depends on the polyP polymer (Figure 12-III). In the absence of polyP, the cells remain on the surface of the hydrogel (Figure 12-III A,B). There, the cells are bulging the surface of the printed hydrogel. Importantly, the cells remain roundish and isolated. Cross fractures showed that the scattered cells have a rounded morphology; they remain isolated (Figure 12-III E,F). In contrast, in the hydrogel matrix with polyP, the cells form clusters at the surface of the prints (Figure 12-III C,D), and the lobulated MSC form aggregates, as shown in cross fractures (Figure 12-III G,H). This series of experiments showed that the growth/aggregate pattern of MSC changes from isolated cells to globular to lobular spheres when embedded in the polyP bioink, which is indicative of cell differentiation.^[131]

The master genes that control the switch in MSC toward cartilage and bone differentiation are the two transcription factors RUNX2 (runt-related transcription factor 2) and Sox9 (SRY-box transcription factor 9).^[132,133] Gene expression studies revealed a distinct increase in the expression ratio between RUNX2 and Sox9 in cells growing in polyP-supplemented hydrogel, reflecting an increased propensity for differentiation. In addition, the morphogenetic activity of the MSC in the polyP-enriched matrix is underpinned by the finding that the MSC in this polyP hydrogel show a strong induction of the expression of the ALP gene.^[129]

4.1.4. In Vivo Studies

The proof-of-concept implying that the precursor for crystalline bone (HA) formation originates from an amorphous precursor,^[60] an initial amorphous calcium phosphate phase (ACP), was tested in in vivo studies. ACP transforms into the crystalline apatite.^[134] Earlier it was established that ACP is stabilized by polyP ($\approx 15\text{--}20\%$ by weight).^[135] ACP was found to be superior to crystalline β -TCP in the calvarial defect regeneration model in rats.^[135] Building on the strong evidence for a significant ACP content in crystalline mature bone by the Posner group,^[136] a modeling approach revealed that polyP chains can protrude between the Posner molecules and thereby stabilize the ACP phase. Therefore, it was advisable to determine the regenerative effect of amorphous versus crystalline calcium phosphate precursor in vivo.^[137] Again, the calvarial defect model (New Zealand White rabbits) was applied. The Ca-phosphate minerals (see Section 4.1.1.), crystalline β -TCP, crystalline Ca-phosphate (CCP [with 5% (w/w) polyP]) and amorphous Ca-phosphate (ACP [stabilized with 15% (w/w) polyP]) were encapsulated into microspheres with poly(D,L-lactide-co-glycolide) (PLGA) and applied into the defect. After a healing period of 6 weeks, the animals were sacrificed and assessed. A comparison of the histology of the regenerating areas revealed that in the β -TCP series, all microspheres had dropped out of the tissue slices and no signs of regeneration could be observed. The subsequent SEM analyses confirmed that the microspheres project out of the defect in the calvarial bone. In contrast, strong signs of regeneration were already evident in the CCP series (supplemented with low amounts of polyP); even new blood vessels could be identified. These results from SEM analyses supported the regenera-

tion effect and were underpinned by histological analyses, which showed infiltration of cells into the microspheres and also the presence of regenerative tissue in their surroundings. In conclusion, the ACP-supplemented microspheres showed the strongest regeneration potency.^[137]

Bone regeneration, like regeneration of skin tissue (see Section 4.3.), is a highly energy-dependent process. This is reflected in a sharp increase in the ATP content in the callus during fracture healing, indicating intensive energy metabolism in the newly forming bone tissue.^[138] Exploiting the energy-supplying function of polyP as well as its ability to convert into a regeneratively active coacervate upon contact with body fluids, a number of further animal studies have been conducted that confirmed the benefits of polyP and its amorphous polyP nanoparticles in bone healing. It was found that polyP encapsulated in PLGA microspheres (polyP content, 7.26 ± 0.92 wt.%) significantly enhanced bone regeneration in critical-size calvarial defects (rat) compared to β -TCP used as a reference material.^[139] Bone mineralization was accompanied by strongly upregulated expression of collagen type I and the marker protein ALP in the polyP implant area. Nanoindentation revealed a hardness/Young's modulus of the newly formed tissue around the polyP implant close to that of calvarial bone within a 56-day healing period.^[139] In another study, polyP integrated in a *N,O*-CMC matrix was studied, again using the rat calvarial defect model.^[140] Both polymers were linked together via Ca^{2+} . The microspheres composed of polyP (20 mg mL^{-1}), *N,O*-CMC (60 mg mL^{-1}), and alginate (60 mg mL^{-1}) were found to be superior in their regeneration-inducing activity to microspheres containing β -TCP or β -TCP together with silica. With a hardness/Young's modulus of 1175 kPa, the mechanical properties of the regenerating areas exceeded those around the β -TCP and β -TCP/silica reference implants by a factor of 2–3 and almost reached those of the pre-existing bone (1840 kPa).^[140] Nanoparticles prepared from the strontium salt of polyP showed even higher mineralization-inducing activity than the Ca-polyP particles.^[141] The stronger osteogenic effect of the amorphous Sr-polyP particles was explained by the finding that these particles only slightly upregulated the expression of sclerostin compared to ALP in contrast to the Ca-polyP particles.^[141] This antagonist of Wnt/ β -catenin signaling suppresses the differentiation and mineralization of bone cells.^[142] In the rat calvaria, the bone defect was almost completely restored after an implantation period of 12 weeks.^[141]

Recently, in a first-in-human clinical trial the safety, feasibility, and osteoinductivity of Ca-polyP-NP have been evaluated.^[143] In this single-blinded, parallel, prospective pilot study, Ca-polyP-NP has been applied either alone (1 g in 1.5 mL saline) or in combination with biphasic calcium phosphate (BCP; composed of 60% HA and 40% β -TCP) (1 g Ca-polyP-NP and 2 g BCP in 3–5 mL saline) for alveolar cleft repair. Based on the results, it was concluded that Ca-polyP-NP is a safe material. None of the patients developed allergic reactions or showed other local or systemic adverse effects.

It should be noted that polyP has also been recognized as safe for use as a food additive by the US Food and Drug Administration (FDA) and the European Union (EU); it is listed under the E-numbers E 452(i) (Na-polyP), E 452(iii) (Na/Ca-polyP) and E 452(iv) (Ca-polyP).^[144] Furthermore, this polymer shows no carcinogenicity, no reproductive or developmental toxicity, and no

genotoxicity.^[138] The LD₅₀ for polyP in rats and mice is very low at >2000 mg kg⁻¹.^[145]

4.2. Enhanced Growth Of Human Chondrocytes Onto Cartilage

One reason for the limited regeneration capacity of cartilage is the low proportion of chondrocytes/MSC in this tissue. Only a proportion of 1–5% chondrocytes has been estimated.^[146] In addition, the blood supply is very low. It was therefore conceivable to test if polyP, which is normally supplied by the platelets, could substitute for this polymer in ameliorating cartilage damage.

Already in 2012^[147] it was reported that polyP (the exact formulation was not given) with the physiological chain length of 45 P_i units stimulates the synthesis of collagens and glycosaminoglycans in chondrocytes; in comparison, phosphate or pyrophosphate had no beneficial effect. These positive effects could be confirmed with cartilage explants cultivated in vitro. Even in vivo (guinea pigs) it could be demonstrated that intra-articular injections of polyP significantly improved the osteoarthritis-outcome score.

In a subsequent study, polyP was investigated in vitro in the formulation of amorphous magnesium (Mg) salts, Mg-polyP-NP.^[148] This decision was based on the findings that magnesium is an essential cofactor for a number of enzymes and other functional proteins in the human body.^[149] A deficiency in this element leads to neuromuscular, cardiac, or nervous disorders. Mg-polyP-NP were encapsulated into *N,O*-CMC, and alginate and fabricated into tissue units with Young's modulus/stiffness comparable to those of in vivo samples.^[148] Gene expression studies revealed that chondrocytes seeded on these specimens strongly upregulate the expression of both collagen type II and aggrecan, the major proteoglycan present in the articular cartilage.

A Ca-polyP-NP-containing porous cryogel with cartilage-like viscoelastic properties, prepared from polyP, karaya gum, and polyvinyl alcohol by Ca²⁺-mediated ionic gelation and intermolecular cross-linking, has been evaluated in an animal study.^[150] Implants in rat muscle with microspheres containing this material were found to be replaced by granulation tissue after just 2–4 weeks of implantation.^[142] In vitro, it was shown that the Ca-polyP-NP, generated in situ within this cryogel are converted into the biologically active coacervate upon contact with body fluid, allowing human MSC to invade and proliferate.

4.3. Wound Healing, an Energy-Consuming Repair Process

The skin, as the body's largest organ, protects the individual from bacteria, regulates body temperature, and also controls sensations such as touch and pain. Since the skin is the effective barrier between the environment and the internal milieu, it determines and maintains the body's homeostasis and thus the survival of the organism.^[151] It is therefore essential that the repair and regeneration capacity of the skin is maintained. Wound healing is a physiological reaction of the body to tissue injury and is complex. It involves an interplay between different cell types, cytokines, mediators, and the vascular system. It is important that both initial vasoconstriction of blood vessels and platelet aggregation progress and lead to cessation of bleeding. In gen-

eral, wound healing is subdivided into four phases: Hemostasis, inflammation, proliferation (granulation), and remodeling (Figure 13-1).^[152]

4.3.1. Hemostasis

Hemostasis is a process by which bleeding is stopped and clotting occurs, causing blood to form from a liquid into a gel. The blood vessels constrict and reduce bleeding. Subsequently, the platelets stick together to form a plug and (temporarily) seal the vessel wall. Finally, coagulation (blood clotting) occurs, a process in which a series of enzyme-driven reactions is activated, finally leading to a fibrin mesh produced around the platelet plug.

Ca²⁺ is a central ion controlling hemostasis during vascular injury.^[153] The von Willebrand factor interacts with the platelets leading to an increase in the free Ca²⁺ concentration. Ca²⁺ causes the activation of several coagulation factors, such as Factor XIII. This ion is responsible for cross-linking fibrin clots and maintaining the clot architecture. Factor XIII is associated with a protransglutaminase complex, which, together with thrombin and Ca²⁺, activates the final stage of the clotting cascade.^[154]

It has been proposed that polyP modulates blood clotting,^[32] a view that has been disputed.^[155] The problem is that the degree of binding (chelate formation) of the respective cations to the polyP anion has often not been taken into account. Therefore, the cation exchange reactions of Na⁺, Mg²⁺, and Ca²⁺ have to be considered in detail. Also, chelating Ca²⁺ from the system effectively prevents blood clotting.^[156] In addition, the chain length of the polyP used for the particular study is an important issue.^[90] These authors stress that the potency of polyP depends on the chain length of the polymer and highlight the distinctive physiological roles of short-chain polyP released from the platelet-dense granules and long-chain polyP produced in bacteria.

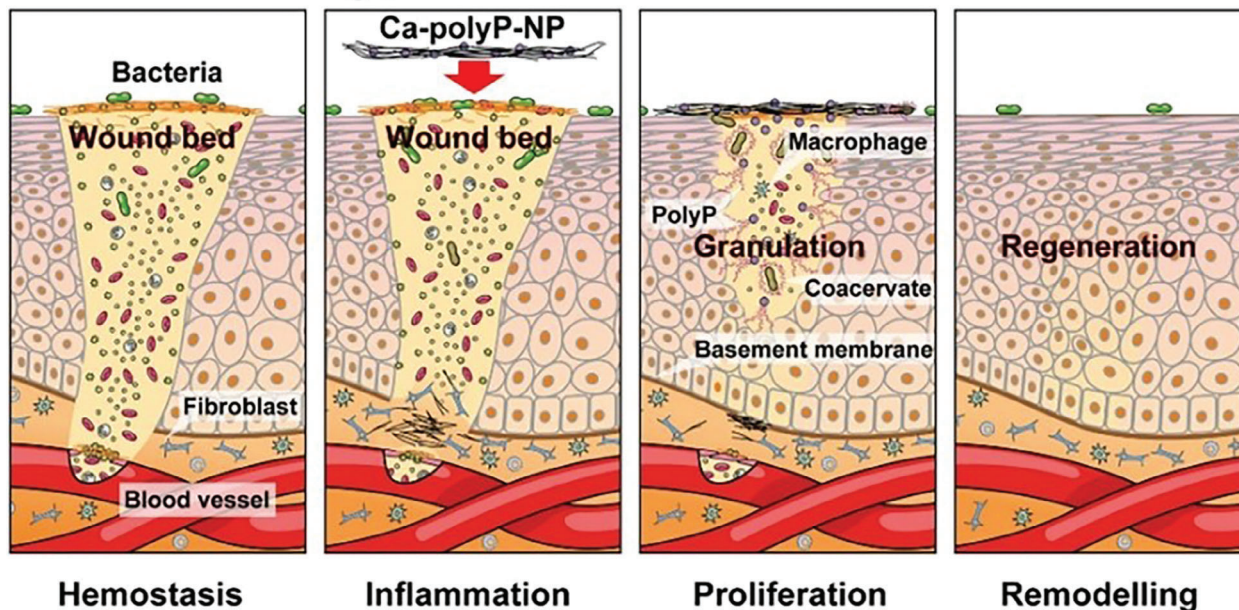
4.3.2. Inflammation

During the inflammation phase, immune cells clean the injured site by phagocytosis, thereby removing damaged cells, pathogens, and bacteria, and neutrophils, macrophages, and monocytes migrate into the wound area. It has been shown that polyP (of the physiological chain length 60–100 P_i units) promotes the differentiation of macrophages and fibrocytes and mediates wound healing anabolically.^[89] In addition, monocytes are stimulated by polyP to differentiate into fibrocytes and macrophages. Furthermore, polyP supports antibacterial processes during the inflammation phase by directly affecting both some Gram-positive bacteria and some Gram-negative bacteria.^[157]

4.3.3. Proliferation (Granulation)

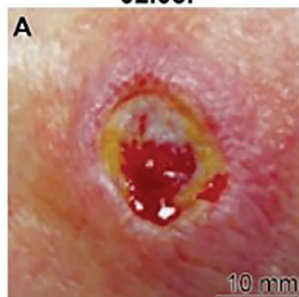
This phase in particular is very metabolic energy consuming.^[158] During this period, angiogenesis, the growth of blood vessels from the existing and accumulating cells, must have to develop. Especially, fibroblasts have to migrate to the injured site, even more fibroblasts have to differentiate to myofibroblasts,

I. Wound healing phases

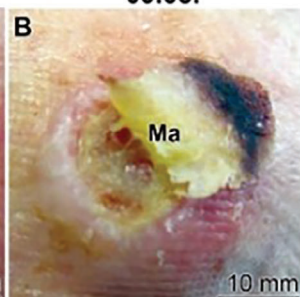


II. polyP-collagen mat

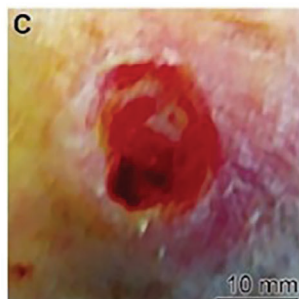
Initial medical picture (100%)
02.03.



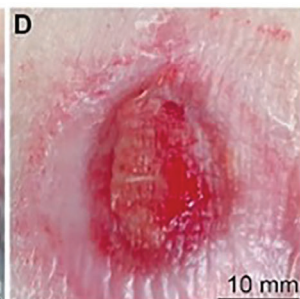
09.03.



Mat replacement



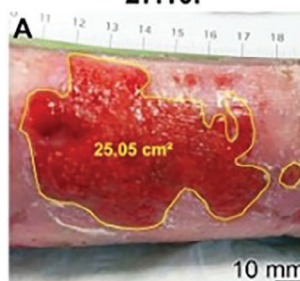
09.03.



Treatment completed
07.07.

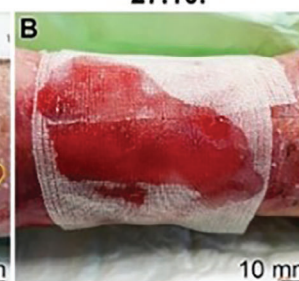
III. polyP-hydrogel

Initial picture (100%)
27.10.



4+3 mo: standard therapy
then: polyP hydrogel

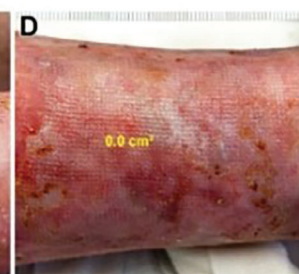
27.10.



polyP hydrogel



polyP hydrogel
02.11.



Wound closure
09.11.

Figure 13. Successful proof-of-concept trials with polyP. I) The four phases of wound healing. II) Application of polyP embedded in a collagen mat (the dates when the respective treatments were performed are also given). A) Initial clinical picture. The treatment started with the collagen-polyP mat. B,C) Then, the bulged mat (Ma) was replaced; a marginal epithelial rim developed around the wound. (D) Termination of the polyP treatment. III) Accelerated treatment of manifested superficial erosions on a prurigo eczema using the polyP ($600 \mu\text{g mL}^{-1}$ Na-polyP and $60 \mu\text{g mL}^{-1}$ Ca-polyP-NP) loaded hydrogel. A) Initial clinical picture. B) Covering of the wound with the polyP hydrogel and overlaying with a neutral gauze. C,D) During the treatment, the wound area was reduced to 19.5% of the initial size and finally even completely. II) Reproduced under the terms of the CC BY 4.0 DEED license.^[28] Copyright 2022, Ivyspring International Publisher. III) Reproduced with permission.^[152] Copyright 2022, Elsevier Ltd.

(such as ATP or coenzyme A), which supply energy via their energy-rich bonds.^[191] As shown here, polyP also meets these requirements as it delivers the metabolic energy (ATP) needed for kinases, as well as for heat shock proteins and the extracellular matrix structural organization.

It has been a long way to uncover the biological and biochemical basis of regeneration. Already in the Second Book of Aristotle entitled “History of Animals” (cited from ref. [192]) he wrote in 350 B.C. “...The tails of saurian and of serpents, if they are cut off, will grow again.” Revolutionary was the discovery that the cnidarian Hydra has the potency to regenerate missing parts after the individuals had been dissected.^[193] With the inclusion of genetics,^[194] the causal analytical line of thinking was implemented to understand regeneration. In the 1985s, stem cell biology was flourishing with the discovery that stem cells reside in adult tissues, where they have a robust regenerative capacity in vivo while being rapidly lost in culture.^[195] Growth factors have been found to regulate cell functions and stimulate their proliferation and differentiation, often in combination with other growth factors such as cytokines. In turn, the concept of harnessing stem cells for biomedical purposes became more realistic.^[196]

There is increasing evidence that bioenergetics, i.e., the adjustment of energy metabolism, is crucial for the progression of stem cell differentiation.^[197] Of particular importance is the Sirtuin 1 (SIRT1) cycle, which directly links the cellular metabolic status to gene expression and regulates glucose and lipid metabolism in the liver and other organs, promotes fat mobilization and stimulates remodeling of brown fat.^[198] In addition, the nutrient sensor SIRT1 promotes bioenergetic pathways in stem cell activation and regulates the autophagic flux in response AMP-activated protein kinase.^[199] Also worth mentioning is that the reduction of ATP supply reduces pluripotency.^[200]

With the application for wound healing in patients, polyP has successfully mastered the proof-of-concept phase. It was also a significant advancement to show that polyP accelerates the regeneration of bone and cartilage defects in vitro and in animals. For all these healing applications, there is a common denominator: the lack of metabolic energy during the costly regeneration processes.

Often the ECM has been explained in terms of supramolecular assemblies organized from small, modular subunits forming homopolymers and heteropolymers.^[201,202] The energetics of supramolecular fabricating can only partially be explained in terms of free energy minimization.^[202] Only after feeding the system with ATP, the dynamics of the migration of polymers can be kept running and self-assembly interactions of macromolecules can continue.^[202]

In conclusion, this review outlines the biomedical potential of polyP, especially for regenerative processes aimed at repairing organs that are poor in cells. The formulation of polyP, in the NP form, turned out to be advantageous because the application can be carefully targeted and the high surface-to-volume ratio of the particles allows a shaping of the pharmacokinetic profile. For polyP, the breakthrough came after the successful elaboration of the method to prepare amorphous polyP-NP in a bioinspired way as synthesized in the acidocalcisomes or dense granules.^[59] As with any functionally active bio-inorganic material, polyP must be present in an amorphous form in the NP.^[59,203] To become biomedically active, the NP fabricated must have a ζ potential

that allows adsorption to the cell surfaces in the target organ and also endocytotic uptake, as elaborated with Ca-polyP-NP.^[204] Here, polyP has the distinguished property of changing from the NP state to the coacervate phase,^[14] whereby the “biologically inert” NP are converted into a functionally active form. In the second step, the polyP coacervate undergoes enzymatic hydrolysis or phosphotransfer mediated by ALP and ADK to generate extracellular metabolic energy that speeds up regeneration processes, as highlighted for bone and wounds.

It is hoped that this review will contribute to a further understanding of the secrets of physiological regeneration induced by nanoparticles formed by polyP.

Acknowledgements

The authors thank Mr. Gunnar Glasser (Department of Physical Chemistry of Polymers, Max Planck Institute for Polymer Research, Mainz; Germany) for continuous and very expert support. W.E.G.M. is the holder of an ERC Advanced Investigator Grant (grant number 268476). In addition, W.E.G. M. has obtained three ERC-PoC grants (Si-Bone-PoC, Grant no.: 324564; MorphoVES-PoC, Grant no.: 662486; and ArthroDUR, Grant no.: 767234). In addition, this work was supported by grants from the International Human Frontier Science Program (RG-333/96-M) and the Bundesministerium für Bildung und Forschung (Grant no. 13GW0403A/B – SKIN-ENERGY)

Open access funding enabled and organized by Projekt DEAL.

Conflict of Interest

The authors declare no conflict of interest.

Author Contributions

M.N. and S.W. performed the experiments, analyzed the results, and revised the original draft of the manuscript. W.E.G.M., H.C.S., and X.H.W. wrote the manuscript and supervised the whole project. W.E.G.M. and X.H.W. provided the resources. All authors discussed mutually and intensely the results and commented on the manuscript.

Keywords

biomaterials, coacervate, energy storage, inorganic polyphosphate, metabolic energy, nanoparticles, regenerative activity

Received: October 20, 2023

Revised: January 29, 2024

Published online: March 12, 2024

- [1] I. S. Kulaev, V. M. Vagabov, T. V. Kulakovskaya, L. P. Lichko, N. A. Andreeva, L. V. Trilisenko, *Biochem. (Mosc.)* **2000**, 65, 271.
- [2] M. R. Brown, A. Kornberg, *Proc. Natl. Acad. Sci. USA* **2004**, 101, 16085.
- [3] W. E. G. Müller, H. C. Schröder, X. H. Wang, *Biochem. – Elements Biochem.* **2019**, 41, 22.
- [4] H. C. Schröder, W. E. G. Müller (Eds.), *Inorganic Polyphosphates – Biochemistry, Biology, Biotechnology*, Springer Press, Heidelberg, Germany **1999**.
- [5] I. S. Kulaev, V. Vagabov, T. Kulakovskaya, *The Biochemistry of Inorganic Polyphosphates*, John Wiley, Chichester, England **2004**.

- [6] N. N. Rao, M. R. Gómez-García, A. Kornberg, *Annu. Rev. Biochem.* **2009**, *78*, 605.
- [7] T. Kulakovskaya, E. Pavlov, E. N. Dedkova (Eds.), *Inorganic Polyphosphates in Eukaryotic Cells*, Springer International Publishing, Basel, Switzerland **2016**.
- [8] K. Lohmann, *Naturwissenschaften* **1929**, *17*, 624.
- [9] K. Lohmann, *Biochem. Z.* **1931**, *233*, 460.
- [10] R. Jenner, J. Brachet, *Enzymologia* **1944**, *11*, 22.
- [11] G. Schmidt, L. Hecht, S. J. Thannhauser, *J. Biol. Chem.* **1946**, *166*, 775.
- [12] J. P. Ebel, G. Dirheimer, A. Stahl, S. Feller, *Quelques aspects nouveaux de la biochimie des polyphosphates inorganiques. Composés organiques du phosphate*, Coll. Nat. du CNRS, CNRS, Paris **1966**, p. 289.
- [13] E. Liss, P. Langen, *Biochem. Z.* **1960**, *333*, 193.
- [14] W. E. G. Müller, S. F. Wang, E. Tolba, M. Neufurth, M. Ackermann, R. Muñoz-Espí, I. Lieberwirth, G. Glasser, H. C. Schröder, X. H. Wang, *Small* **2018**, *14*, 1801170.
- [15] X. Wang, C. Shi, J. Mo, Y. Xu, W. Wei, J. Zhao, *Angew. Chem. Int. Ed. Engl.* **2020**, *59*, 2679.
- [16] L. Achbergerová, J. Nahálka, *Microb. Cell Fact.* **2011**, *10*, 63.
- [17] W. E. G. Müller, H. C. Schröder, X. H. Wang, *Chem. Rev.* **2019**, *119*, 12337.
- [18] G. Leyhausen, B. Lorenz, H. Zhu, W. Geurtsen, R. Bohnensack, W. E. G. Müller, H. C. Schröder, *J. Bone Mineral. Res.* **1998**, *13*, 803.
- [19] S. Omelon, J. Georgiou, Z. J. Henneman, L. M. Wise, B. Sukhu, T. Hunt, C. Wynnickyj, D. Holmyard, R. Bielecki, M. D. Grynepas, *PLoS One* **2009**, *4*, e5634.
- [20] W. E. G. Müller, X. H. Wang, B. Diehl-Seifert, K. Kropf, U. Schloßmacher, I. Lieberwirth, G. Glasser, M. Wiens, H. C. Schröder, *Acta Biomater.* **2011**, *7*, 2661.
- [21] K. Shimizu, J. Cha, G. D. Stucky, D. E. Morse, *Proc. Natl. Acad. Sci. USA* **1998**, *95*, 6234.
- [22] A. Krasko, B. Lorenz, R. Batel, H. C. Schröder, I. M. Müller, W. E. G. Müller, *Eur. J. Biochem.* **2000**, *267*, 4878.
- [23] X. H. Wang, H. C. Schröder, K. Wang, J. A. Kaandorp, W. E. G. Müller, *Soft Matter* **2012**, *8*, 9501.
- [24] W. E. G. Müller, X. H. Wang, H. C. Schröder, *Progress in Molecular and Subcellular Biology* (Eds.: W. E. G. Müller, X. H. Wang, H. C. Schröder) **55**, Springer Cham, Basel, Switzerland **2017**, p. 187.
- [25] J. van Straelen, F. Geuzebroek, *Energy Procedia* **2011**, *4*, 1500.
- [26] Q. Lian, H. Cao, F. Wang, *Appl. Biochem. Biotechnol.* **2014**, *174*, 2351.
- [27] W. E. G. Müller, H. C. Schröder, M. Neufurth, X. H. Wang, *Mater. Today* **2021**, *51*, 504.
- [28] H. Schepler, M. Neufurth, S. F. Wang, Z. D. She, H. C. Schröder, X. H. Wang, W. E. G. Müller, *Theranostics* **2022**, *12*, 18.
- [29] H. Holmsen, H. J. Weiss, *Annu. Rev. Med.* **1979**, *30*, 119.
- [30] M. H. Fukami, C. A. Dangelmaier, J. S. Bauer, H. Holmsen, *Biochem. J.* **1980**, *192*, 99.
- [31] F. A. Ruiz, C. R. Lea, E. Oldfield, R. Docampo, *J. Biol. Chem.* **2004**, *279*, 44250.
- [32] F. Müller, N. J. Mutch, W. A. Schenk, S. A. Smith, L. Esterl, H. M. Spronk, S. Schmidbauer, W. A. Gahl, J. H. Morrissey, T. Renné, *Cell* **2009**, *139*, 1143.
- [33] J. H. Morrissey, S. H. Choi, S. A. Smith, *Blood* **2012**, *119*, 5972.
- [34] E. Bondy-Chorney, I. Abramchuk, R. Nasser, C. Holinier, A. Denoncourt, K. Baijal, L. McCarthy, M. Khacho, M. Lavallée-Adam, M. Downey, *Cell Rep.* **2020**, *33*, 108318.
- [35] T. V. Kulakovskaya, L. P. Lichko, V. M. Vagabov, I. S. Kulaev, *Biochem. (Mosc.)* **2010**, *75*, 825.
- [36] K. Ahn, A. Kornberg, *J. Biol. Chem.* **1990**, *265*, 11734.
- [37] A. Kornberg, N. N. Rao, D. Ault-Riché, *Annu. Rev. Biochem.* **1999**, *68*, 89.
- [38] E. Partridge, V. Hicks, G. W. Smith, *J. Amer. Chem. Soc.* **1941**, *63*, 454
- [39] D. E. C. Corbridge, *Phosphorus: Chemistry, Biochemistry and Technology*, 6th ed., CRC Press/Taylor & Francis, Boca Raton, Florida, USA **2013**, p. 234.
- [40] C. F. Callis, F. Clayton, J. R. Van Wazer, P. G. Arvan, *Chem. Rev.* **1954**, *54*, 777.
- [41] S. Ramakrishnan, B. Asady, R. Docampo, *Pathogens* **2018**, *7*, 33.
- [42] R. Docampo, G. Huang, *J. Eukaryot. Microbiol.* **2022**, *69*, 12899.
- [43] Y. Desfougères, H. Neumann, A. Mayer, *J. Cell Sci.* **2016**, *129*, 2817.
- [44] M. Hothorn, H. Neumann, E. D. Lenherr, M. Wehner, V. Rybin, P. O. Hassa, A. Uttenweiler, M. Reinhardt, A. Schmidt, J. Seiler, A. G. Ladurner, C. Herrmann, K. Scheffzek, A. Mayer, *Science* **2009**, *324*, 513.
- [45] Z. Guan, J. Chen, R. Liu, Y. Chen, Q. Xing, Z. Du, M. Cheng, J. Hu, W. Zhang, W. Mei, B. Wan, Q. Wang, J. Zhang, P. Cheng, H. Cai, J. Cao, D. Zhang, J. Yan, P. Yin, M. Hothorn, Z. Liu, *Nat. Commun.* **2023**, *14*, 718.
- [46] J. J. Verhoef, A. D. Barendrecht, K. F. Nickel, K. Dijkxhoorn, E. Kenne, L. Labberton, O. J. McCarty, R. Schiffelers, H. F. Heijnen, A. P. Hendrickx, H. Schellekens, M. H. Fens, S. de Maat, T. Renné, C. Maas, *Blood* **2017**, *129*, 1707.
- [47] M. K. Nayak, M. Ghatge, G. D. Flora, N. Dhanesha, M. Jain, K. R. Markan, M. J. Potthoff, S. R. Lentz, A. K. Chauhan, *Blood* **2021**, *137*, 1658.
- [48] J. S. Straub, M. S. Nowotarski, J. Lu, T. Sheth, S. Jiao, M. P. A. Fisher, M. S. Shell, M. E. Helgeson, A. Jerschow, S. Han, *Proc. Natl. Acad. Sci. USA* **2023**, *120*, 2206765120.
- [49] R. G. Pearson, *J. Am. Chem. Soc.* **1963**, *85*, 3533.
- [50] X. H. Wang, H. Schepler, M. Neufurth, S. Wang, H. C. Schröder, W. E. G. Müller, in *Inorganic Polyphosphates – From Basic Research to Medical Application* (Eds.: W. E. G. Müller, H. C. Schröder, P. Suess, X. H. Wang), Springer Nature, Cham, Switzerland **2022**, pp. 51–82.
- [51] A. Momeni, M. J. Filiaggi, *Acta Biomater.* **2016**, *41*, 328.
- [52] W. E. G. Müller, M. Neufurth, I. Lieberwirth, S. F. Wang, H. C. Schröder, X. H. Wang, *Mater. Today Bio.* **2022**, *16*, 100404.
- [53] W. E. G. Müller, S. F. Wang, M. Neufurth, H. C. Schröder, X. H. Wang, in *Bioinformatics and Biomedical Engineering* (Eds.: I. Rojas, O. Valenzuela, F. R. Ruiz, L. J. Herrera, F. Ortuño), IWBBIO 2023, Gran Canaria, Spain, **2023**, Proceedings, Part I, p. 542.
- [54] P. Y. Shih, J. Y. Ding, S. Y. Lee, *Mater. Chem. Phys.* **2003**, *80*, 391.
- [55] A. Khoshmanesh, P. L. Cook, B. R. Wood, *Analyst* **2012**, *137*, 3704.
- [56] D. M. Pickup, R. J. Newport, E. R. Barney, J. Y. Kim, S. P. Valappil, J. C. Knowles, *J. Biomater. Appl.* **2014**, *28*, 1226.
- [57] L. C. Chow, in *Octacalcium Phosphate* (Eds.: L. C. Chow, E. D. Eanes), Karger, Switzerland **2001**, *18*, 94.
- [58] I. Greenwald, *J. Biol. Chem.* **1942**, *143*, 703.
- [59] W. E. G. Müller, E. Tolba, H. C. Schröder, S. F. Wang, G. Glaßer, R. Muñoz-Espí, T. Link, X. H. Wang, *Mater. Lett.* **2015**, *148*, 166.
- [60] L. Addadi, S. Weiner, *Phys. Scr.* **2014**, *89*, 098003.
- [61] X. H. Wang, H. C. Schröder, W. E. G. Müller, *J. Mat. Chem. B* **2018**, *6*, 2385.
- [62] J. J. Grzesiak, M. D. Pierschbacher, *J. Clin. Invest.* **1995**, *95*, 227.
- [63] M. Mailland, R. Waelchli, M. Ruat, H. G. Boddeke, K. Seuwen, *Endocrinology* **1997**, *138*, 3601.
- [64] W. E. G. Müller, H. Schepler, E. Tolba, S. F. Wang, M. Ackermann, R. Muñoz-Espí, S. C. Xiao, R. W. Tan, Z. D. She, M. Neufurth, H. C. Schröder, X. H. Wang, *J. Mater. Chem. B* **2020**, *8*, 5892.
- [65] G. MacLennan, C. A. Beevers, *Acta Cryst.* **1956**, *9*, 187.
- [66] F. Sadeghi, A. Fayazi, *Ind. Eng. Chem. Res.* **2012**, *51*, 1093.
- [67] M. Shimaya, T. Muneta, S. Ichinose, K. Tsuji, I. Sekiya, *Osteoarthr. Cartil.* **2010**, *18*, 1300.
- [68] J. You, Y. Zhang, Y. Zhou, *Front. Bioeng. Biotechnol.* **2022**, *10*, 928799.
- [69] L. Xie, U. Jakob, *J. Biol. Chem.* **2019**, *294*, 2180.

- [70] M. J. Gray, W. Y. Wholey, N. O. Wagner, C. M. Cremers, A. Mueller-Schickert, N. T. Hock, A. G. Krieger, E. M. Smith, R. A. Bender, J. C. Bardwell, U. Jakob, *Mol. Cell.* **2014**, *53*, 689.
- [71] C. M. Cremers, D. Knoefler, S. Gates, N. Martin, J. U. Dahl, J. Lempart, L. Xie, M. R. Chapman, V. Galvan, D. R. Southworth, U. Jakob, *Mol. Cell.* **2016**, *63*, 768.
- [72] V. Ferrucci, D. Y. Kong, F. Asadzadeh, L. Marrone, A. Boccia, R. Siciliano, G. Criscuolo, C. Anastasio, F. Quarantelli, M. Comegna, I. Pisano, M. Passariello, I. Iacobucci, R. D. Monica, B. Izzo, P. Cerino, G. Fusco, M. Viscardi, S. Brandi, B. M. Pierri, G. Borriello, C. Tiberio, L. Atripaldi, M. Bianchi, G. Paoletta, E. Capoluongo, G. Castaldo, L. Chiariotti, M. Monti, C. De Lorenzo, et al., *Sci. Signal.* **2021**, *14*, eabe5040.
- [73] L. Harhaus, J. J. Huang, S. W. Kao, Y. L. Wu, G. A. Mackert, B. Höner, M. H. Cheng, U. Kneser, C. M. Cheng, *J. Cell. Mol. Med.* **2015**, *19*, 1273.
- [74] S. F. Wang, X. H. Wang, M. Neufurth, E. Tolba, H. Schepler, S. C. Xiao, H. C. Schröder, W. E. G. Müller, *Molecules* **2020**, *25*, 5210.
- [75] L. C. Ponomarev, J. Ksiazkiewicz, M. W. Staring, A. Luttun, A. Zwijsen, *Int. J. Mol. Sci.* **2021**, *22*, 6364.
- [76] J. B. Sipe, J. Zhang, C. Waits, B. Skikne, R. Garimella, H. C. Anderson, *Bone* **2004**, *35*, 1316.
- [77] S. H. Yun, E. H. Sim, R. Y. Goh, J. I. Park, J. Y. Han, *BioMed. Res. Int.* **2016**, *2016*, 9060143.
- [78] L. Locatelli, A. Colciago, S. Castiglioni, J. A. Maier, *Front. Bioeng. Biotechnol.* **2021**, *9*, 716184.
- [79] J. I. Weitz, J. C. Fredenburgh, *Blood* **2017**, *129*, 1574.
- [80] S. Luo, F. A. Ruiz, S. N. Moreno, *Mol. Microbiol.* **2005**, *55*, 1034.
- [81] A. Sharda, R. Flaumenhaft, *F1000Research* **2018**, *7*, 236.
- [82] R. Tyagi, S. Chakraborty, S. J. Tripathi, I. R. Jung, S. F. Kim, S. H. Snyder, B. D. Paul, *iScience* **2023**, *26*, 107199.
- [83] B. Lorenz, J. Münkner, M. P. Oliveira, A. Kuusksalu, J. M. Leitão, W. E. G. Müller, H. C. Schröder, *Biochim. Biophys. Acta* **1997**, *1335*, 51.
- [84] S. A. Smith, N. J. Mutch, D. Baskar, P. Rohloff, R. Docampo, J. H. Morrissey, *Proc. Natl. Acad. Sci. USA* **2006**, *103*, 903.
- [85] O. Inoue, K. Suzuki-Inoue, O. J. McCarty, M. Moroi, Z. M. Ruggeri, T. J. Kunicki, Y. Ozaki, S. P. Watson, *Blood* **2006**, *107*, 1405.
- [86] S. Lickert, K. Selcuk, M. Kenny, J. L. Mehl, S. M. Früh, M. A. Burkhardt, J. D. Studt, I. Schoen, V. Vogel, *bioRxiv* **2020**, <https://doi.org/10.1101/2020.04.20.050708>.
- [87] C. Navarro-Requena, S. Pérez-Amodio, O. Castaño, E. Engel, *Nanotechnology* **2018**, *29*, 395102.
- [88] T. Ito, S. Yamamoto, K. Yamaguchi, M. Sato, Y. Kaneko, S. Goto, Y. Goto, I. Narita, *J. Biol. Chem.* **2020**, *295*, 4014.
- [89] P. M. Suess, L. E. Chinea, D. Pilling, R. H. Gomer, *J. Immunol.* **2019**, *203*, 493.
- [90] J. Roewe, S. Walachowski, A. Sharma, K. A. Berthiaume, C. Reinhardt, M. Bosmann, *Front. Immunol.* **2022**, *13*, 980733.
- [91] A. Di Daniele, Y. Antonucci, S. Campello, *Biol. Direct* **2022**, *17*, 8.
- [92] S. Yu, L. Yu, *FEBS J.* **2022**, *289*, 7246.
- [93] R. A. Proctor, J. A. Textor, J. M. Vann, D. F. Mosher, *Infect. Immun.* **1985**, *47*, 629.
- [94] W. E. G. Müller, E. Tolba, Q. Feng, H. C. Schröder, J. S. Markl, M. Kokkinopoulou, X. H. Wang, *J. Cell Sci.* **2015**, *128*, 2202.
- [95] S. Walenta, J. Dötsch, W. Mueller-Klieser, *Eur. J. Cell Biol.* **1990**, *52*, 389.
- [96] U. Sharma, D. Pal, R. Prasad, *Indian J. Clin. Biochem.* **2014**, *29*, 269.
- [97] B. Lorenz, H. C. Schröder, *Biochim. Biophys. Acta* **2001**, *1547*, 254.
- [98] F. A. Kiani, S. Fischer, *Proc. Natl. Acad. Sci. USA* **2014**, *111*, E2947.
- [99] N. Kurebayashi, T. Kodama, Y. Ogawa, *J. Biochem.* **1980**, *88*, 871.
- [100] W. E. G. Müller, M. Ackermann, E. Tolba, M. Neufurth, I. Ivetač, M. Kokkinopoulou, H. C. Schröder, X. H. Wang, *Biochem. J.* **2018**, *475*, 3255.
- [101] J. W. F. Nicholls, J. P. Chin, T. A. Williams, T. M. Lenton, V. O'Flaherty, J. W. McGrath, *Front. Microbiol.* **2023**, *14*, 1239189.
- [102] C. H. Chung, E. E. Golub, E. Forbes, T. Tokuoka, I. M. Shapiro, *Calcif. Tissue Int.* **1992**, *51*, 305.
- [103] C. Venkata, R. Kashyap, J. C. Farmer, B. Afessa, *J. Intens. Care* **2013**, *1*, 9.
- [104] R. Simman, J. Haluschak, S. Jackson, *J. Am. Col. Certif. Wound Spec.* **2010**, *2*, 28.
- [105] S. Serbest, U. Tiftikci, H. B. Tosun, S. A. Gumustas, A. Uludag, *Ther. Clin. Risk Manag.* **2016**, *12*, 1095.
- [106] G. S. Baht, L. Vi, B. A. Alman, *Curr. Osteoporos. Rep.* **2018**, *16*, 138.
- [107] C. K. Sen, *Adv. Wound Care (New Rochelle)* **2019**, *8*, 39.
- [108] E. Tolba, W. E. G. Müller, B. M. A. El-Hady, M. Neufurth, F. Wurm, S. F. Wang, H. C. Schröder, X. H. Wang, *J. Mat. Chem. B* **2016**, *4*, 376.
- [109] W. E. G. Müller, M. Neufurth, H. Ushijima, R. Muñoz-Espí, L. K. Müller, S. F. Wang, H. C. Schröder, X. H. Wang, *Dent. Mater.* **2022**, *38*, 2014.
- [110] S. Vimalraj, *Gene* **2020**, *754*, 144855.
- [111] W. N. Addison, F. Azari, E. S. Sørensen, M. T. Kaartinen, M. D. McKee, *J. Biol. Chem.* **2007**, *282*, 15872.
- [112] W. E. G. Müller, E. Tolba, H. C. Schröder, R. Muñoz-Espí, B. Diehl-Seifert, X. H. Wang, *Acta Biomater.* **2016**, *31*, 358.
- [113] J. Filipowska, K. A. Tomaszewski, Ł. Niedźwiedzki, J. A. Walocha, T. Niedźwiedzki, *Angiogenesis* **2017**, *20*, 291.
- [114] I. Silva Barreto, S. Le Cann, S. Ahmed, V. Sotiriou, M. J. Turunen, U. Johansson, A. Rodriguez-Fernandez, T. A. Grunewald, M. Liebi, N. C. Nowlan, H. Isaksson, *Adv. Sci. (Weinh.)* **2020**, *7*, 2002524.
- [115] A. A. Bunaciu, E. G. Udriștioiu, H. Y. Aboul-Enein, *Crit. Rev. Anal. Chem.* **2015**, *45*, 289.
- [116] R. Sautchuk Jr., R. A. Eliseev, *Bone Rep.* **2022**, *16*, 101594.
- [117] P. Li, X. Bian, C. Liu, S. Wang, M. Guo, Y. Tao, B. Huo, *Cell Calcium* **2018**, *71*, 45.
- [118] W. Da, L. Tao, Y. Zhu, *Front. Endocrinol. (Lausanne)* **2021**, *12*, 675385.
- [119] X. H. Wang, H. C. Schröder, W. E. G. Müller, *Beilstein J. Nanotechnol.* **2014**, *5*, 610.
- [120] S. Ravindran, A. George, *Exp. Cell Res.* **2014**, *325*, 148.
- [121] J. Q. Feng, L. M. Ward, S. Liu, Y. Lu, Y. Xie, B. Yuan, X. Yu, F. Rauch, S. I. Davis, S. Zhang, H. Rios, M. K. Drezner, L. D. Quarles, L. F. Bonewald, K. E. White, *Nat. Genet.* **2006**, *38*, 1310.
- [122] J. Q. Fen, J. Zhang, S. L. Dallas, Y. Lu, S. Chen, X. Tan, M. Owen, S. E. Harris, M. MacDougall, *J. Bone Miner. Res.* **2002**, *17*, 1822.
- [123] K. Oya, K. Ishida, T. Nishida, S. Sato, M. Kishino, K. Hirose, Y. Ogawa, K. Ikebe, F. Takeshige, H. Yasuda, T. Komori, S. Toyosawa, *Histochem. Cell Biol.* **2017**, *147*, 341.
- [124] J. Jeong, J. H. Kim, J. H. Shim, N. S. Hwang, C. Y. Heo, *Biomater. Res.* **2019**, *23*, 4.
- [125] P. Müller, U. Bulnheim, A. Diener, F. Lüthen, M. Teller, E. D. Klinkenberg, H. G. Neumann, B. Nebe, A. Liebold, G. Steinhoff, J. Rychly, *J. Cell. Mol. Med.* **2008**, *12*, 281.
- [126] H. Tada, E. Nemoto, B. L. Foster, M. J. Somerman, H. Shimauchi, *Bone* **2011**, *48*, 1409.
- [127] J. Wang, R. Wan, Y. Mo, M. Li, Q. Zhang, S. Chien, *Am. J. Surg.* **2010**, *199*, 823.
- [128] H. Liu, Y. Du, J. P. St-Pierre, M. S. Bergholt, H. Autebage, J. Wang, M. Cai, G. Yang, M. M. Stevens, S. Zhang, *Sci. Adv.* **2020**, *6*, eaay7608.
- [129] M. Neufurth, S. F. Wang, H. C. Schröder, B. Al-Nawas, X. H. Wang, W. E. G. Müller, *Biofabrication* **2022**, *14*, 015016.
- [130] M. R. Bordoli, J. Yum, S. B. Breitkopf, J. N. Thon, J. E. Italiano, J. Xiao, C. Worby, S. K. Wong, G. Lin, M. Edenius, T. L. Keller, J. M. Asara, J. E. Dixon, C. Y. Yeo, M. Whitman, *Cell* **2014**, *158*, 1033.
- [131] C. Rauch, E. Feifel, G. Kern, C. Murphy, F. Meier, W. Parson, M. Beilmann, P. Jennings, G. Gstraunthaler, A. Wilmes, *PLoS one* **2018**, *13*, 0203869.

- [132] F. Westhauser, M. Karadjian, C. Essers, A. S. Senger, S. Hagmann, G. Schmidmaier, A. Moghaddam, *PLoS One* **2019**, *14*, 0212799.
- [133] G. Zhou, Q. Zheng, F. Engin, E. Munivez, Y. Chen, E. Sebald, D. Krakow, B. Lee, *Proc. Natl Acad. Sci. USA* **2006**, *103*, 19004.
- [134] L. Wang, G. H. Nancollas, *Chem. Rev.* **2008**, *108*, 4628.
- [135] X. H. Wang, M. Ackermann, S. F. Wang, E. Tolba, M. Neufurth, Q. L. Feng, H. C. Schröder, W. E. G. Müller, *Biomed. Mater.* **2016**, *11*, 035005.
- [136] J. D. Termine, A. S. Posner, *Calcif. Tissue Res.* **1967**, *1*, 8.
- [137] W. E. G. Müller, M. Ackermann, B. Al-Nawas, L. A. R. Righesso, R. Muñoz-Espí, E. Tolba, M. Neufurth, H. C. Schröder, X. H. Wang, *Acta Biomater.* **2020**, *118*, 233.
- [138] K. S. Leung, A. H. Sher, T. S. Lam, P. C. Leung, *J. Bone Joint Surg. Br.* **1989**, *71*, 657.
- [139] X. H. Wang, S. F. Wang, F. He, E. Tolba, H. C. Schröder, B. Diehl-Seifert, W. E. G. Müller, *Adv. Engin. Mat.* **2016**, *8*, 1406.
- [140] W. E. G. Müller, E. Tolba, H. C. Schröder, M. Neufurth, S. F. Wang, T. Link, B. Al-Nawas, X. H. Wang, *J. Mat. Chem. B.* **2015**, *3*, 1722.
- [141] W. E. G. Müller, E. Tolba, M. Ackermann, M. Neufurth, S. F. Wang, Q. L. Feng, H. C. Schröder, X. H. Wang, *Acta Biomater.* **2017**, *50*, 89.
- [142] T. Malinauskas, E. Y. Jones, *Curr. Opin. Struct. Biol.* **2014**, *29*, 77.
- [143] S. A. Alkaabi, D. S. N. Kalla, G. A. Alsabri, A. Fauzi, N. Jansen, A. Tajrin, R. Nurrahma, W. E. G. Müller, H. C. Schröder, X. H. Wang, T. Forouzanfar, M. N. Helder, M. Ruslin, *Pilot Feasibility Stud.* **2021**, *7*, 199.
- [144] European Parliament and of the Council, Regulation (EC) No 1333/2008 of the European Parliament and of the Council of 16 December 2008 on food additives, OJ. **2008**, L354, 16.
- [145] M. Younes, G. Aquilina, L. Castle, K.-H. Engel, P. Fowler, M. J. Frutos Fernandez, P. Fürst, R. Gürtler, T. Husøy, W. Mennes, P. Moldeus, A. Oskarsson, R. Shah, I. Waalkens-Berendsen, D. Wölflé, P. Aggett, A. Cupisti, C. Fortes, G. Kühnle, I. T. Lillegaard, M. Scotter, A. Giarola, A. Rincon, A. Tard, U. Gundert-Remy, *EFSA J.* **2019**, *17*, 5674.
- [146] A. M. Bhosale, J. B. Richardson, *Br. Med. Bull.* **2008**, *87*, 77.
- [147] J.-P. St-Pierre, J. N. De Croos, J. S. Theodoropoulos, M. Petrera, P. Sharma, S. Li, R. M. Pilliar, M. D. Grynypas, R. A. Kandel, presented at *World Congress on Osteoarthritis*, Barcelona, Spain, April **2012**.
- [148] W. E. G. Müller, M. Neufurth, S. F. Wang, E. Tolba, H. C. Schröder, X. H. Wang, *Eur. Cell. Mater.* **2016**, *31*, 174.
- [149] W. Jahnhen-Dechent, M. Ketteler, *Clin. Kidney J.* **2012**, *5*, i3.
- [150] E. Tolba, X. H. Wang, M. Ackermann, M. Neufurth, R. Muñoz-Espí, H. C. Schröder, W. E. G. Müller, *Adv. Sci.* **2018**, *6*, 1801452.
- [151] A. T. Slominski, M. A. Zmijewski, C. Skobowiat, B. Zbytek, R. M. Slominski, J. D. Stekettee, *Adv. Anat. Embryol. Cell Biol.* **2012**, *212*, 1.
- [152] W. E. G. Müller, H. Schepler, M. Neufurth, S. F. Wang, V. Ferrucci, M. Zollo, R. Tan, H. C. Schröder, X. H. Wang, *J. Mat. Sci. Technol.* **2023**, *135*, 170.
- [153] J. C. Kermode, Q. Zheng, E. P. Milner, *Blood* **1999**, *94*, 199.
- [154] D. Varga-Szabo, A. Braun, B. Nieswandt, *J. Thromb. Haemost.* **2009**, *7*, 1057.
- [155] T. L. Lindahl, S. Ramström, N. Boknäs, L. Faxälv, *Biochem. Soc. Trans.* **2016**, *44*, 35.
- [156] M. E. Mikaelsson, in *Coagulation and Blood Transfusion. Developments in Hematology and Immunology*, Vol. 26 (Eds: C. T. S. Sibinga, P. C. Das, P. M. Mannucci), Springer, Boston, MA **1991**, p. 29.
- [157] J. H. Moon, J. H. Park, J. Y. Lee, *Antimicrob. Agents Chemother.* **2011**, *55*, 806.
- [158] S. Narayanan, S. Eliasson Angelstig, C. Xu, J. Grünler, A. Zhao, W. Zhu, N. Landén Xu, M. Stähle, J. Zhang, M. Ivan, R. G. Maltesen, I. R. Botusan, N. Rajamand Ekberg, X. Zheng, S. B. Catrina, *Commun. Biol.* **2020**, *3*, 768.
- [159] P. J. Hollenbeck, A. D. Bershady, O. Y. Pletjushkina, I. S. Tint, J. M. Vasiliev, *J. Cell Sci.* **1989**, *92*, 621.
- [160] G. Majno, G. Gabbiani, B. J. Hirschel, G. B. Ryan, P. R. Statkov, *Science* **1971**, *173*, 548.
- [161] K. Iwanaga, T. Murata, M. Hori, H. Ozaki, *Eur. J. Pharmacol.* **2013**, *702*, 158.
- [162] T. Thuraisingam, Y. Z. Xu, K. Eadie, M. Heravi, M. C. Guiot, R. Greenberg, M. Gaestel, D. Radzioch, *J. Invest. Dermatol.* **2010**, *130*, 278.
- [163] A. Ozcelikkale, J. C. Dutton, F. Grinnell, B. Han, *J. R. Soc. Interface* **2017**, *14*, 20170287.
- [164] S. Gopal, L. Veracini, D. Grall, C. Butori, S. Schaub, S. Audebert, L. Camoin, E. Baudelet, A. Radwanska, S. Beghelli-de la Forest Divonne, S. M. Violette, P. H. Weinreb, S. Rekima, M. Ilie, A. Sudaka, P. Hofman, E. Van Obberghen-Schilling, *Nat. Commun.* **2017**, *8*, 14105.
- [165] W. E. G. Müller, D. Relkovic, M. Ackermann, S. F. Wang, M. Neufurth, A. Paravic-Radicevic, H. Ushijima, H. C. Schröder, X. H. Wang, *Polymers* **2017**, *9*, 300.
- [166] W. E. G. Müller, S. F. Wang, M. Wiens, M. Neufurth, M. Ackermann, D. Relkovic, M. Kokkinopoulou, Q. F. Feng, H. C. Schröder, X. H. Wang, *PLoS One* **2017**, *12*, 0188977.
- [167] H. Sarojini, A. Bajorek, R. Wan, J. Wang, Q. Zhang, A. T. Billeter, S. Chien, *Front. Pharmacol.* **2021**, *12*, 594586.
- [168] H. Sarojini, A. T. Billeter, S. Eichenberger, D. Druen, R. Barnett, S. A. Gardner, N. J. Galbraith, H. C. Polk Jr., S. Chien, *PLoS One* **2017**, *12*, 0174899.
- [169] Y. Mo, H. Sarojini, R. Wan, Q. Zhang, J. Wang, S. Eichenberger, G. J. Kotwal, S. Chien, *Front. Pharmacol.* **2020**, *10*, 1502.
- [170] S. Manaka, N. Tanabe, T. Kariya, M. Naito, T. Takayama, M. Nagao, D. Liu, K. Ito, M. Maeno, N. Suzuki, M. Miyazaki, *FEBS Lett.* **2015**, *589*, 3108.
- [171] D. Sun, W. G. Junger, C. Yuan, W. Zhang, Y. Bao, D. Qin, C. Wang, L. Tan, B. Qi, D. Zhu, X. Zhang, T. Yu, *Stem Cells* **2013**, *31*, 1170.
- [172] J. M. Rhett, S. A. Fann, M. J. Yost, *Tissue Eng. Part B Rev.* **2014**, *20*, 392.
- [173] L. J. Croucher, A. Crawford, P. V. Hatton, R. G. Russell, D. J. Buttle, *Biochim. Biophys. Acta.* **2000**, *1502*, 297.
- [174] T. B. McEwan, R. A. Sophocleous, P. Cuthbertson, K. J. Mansfield, M. L. Sanderson-Smith, R. Sluyter, *Life Sci.* **2021**, *283*, 119850.
- [175] C. Dsouza, M. S. Moussa, N. Mikolajewicz, S. V. Komarova, *Bone Rep.* **2022**, *17*, 101608.
- [176] M. Kyawsoewin, J. Manokawinchoke, W. Namangkalakul, H. Egusa, P. Limraksasin, T. Osathanon, *BDJ Open.* **2023**, *9*, 28.
- [177] K. S. Nebesnaya, A. R. Makhmudov, K. R. Rustamov, N. S. H. Rakhmatullina, S. I. Rustamova, U. Z. Mirkhodjaev, O. S. Charishnikova, R. Z. Sabirov, A. Y. Baev, *Biochim. Biophys. Acta Gen. Subj.* **2024**, *1868*, 130523.
- [178] A. Y. Baev, P. R. Angelova, A. Y. Abramov, in *Inorganic Polyphosphates in Eukaryotic Cells* (Eds: T. Kulakovskaya, E. Pavlov, E. N. Dedkova), Springer International Publishing, Cham, Switzerland **2016**, pp. 115–121.
- [179] M. Maiolino, N. O'Neill, V. Lariccia, S. Amoroso, S. Sylantsev, P. R. Angelova, A. Y. Abramov, *J. Neurosci.* **2019**, *39*, 6038.
- [180] R. Gawri, R. Bielecki, E. W. Salter, A. Zelinka, T. Shiba, G. Collingridge, A. Nagy, R. A. Kandel, *J. Orthop. Res.* **2022**, *40*, 310.
- [181] D. G. Smith, W. J. Mills, R. G. Steen, D. Williams, *Foot Ankle Int.* **1999**, *20*, 258.
- [182] W. K. Stadelmann, A. G. Digenis, G. R. Tobin, *Am. J. Surg.* **1998**, *176-2A*, 265S.
- [183] G. S. Lazarus, D. M. Cooper, D. R. Knighton, R. E. Percoraro, G. Rodeheaver, M. C. Robson, *Wound Repair Regen.* **1994**, *2*, 165.
- [184] C. K. Sen, *Adv. Wound Care* **2021**, *10*, 281.
- [185] B. Dalisson, J. Barralet, *Adv. Healthcare Mater.* **2019**, *8*, 1900764.
- [186] C. C. Ning, S. Logsetty, S. Ghughare, S. Liu, *Burns* **2014**, *40*, 1164.

- [187] A. M. Szpaderska, E. I. Egozi, R. L. Gamelli, L. A. DiPietro, *J. Invest. Dermatol.* **2003**, 120, 1130.
- [188] F. Ajallouéian, N. Nikogeorgos, A. Ajallouéian, M. Fossum, S. Lee, I. S. Chronakis, *Int. J. Biol. Macromol.* **2018**, 108, 158.
- [189] S. Werner, T. Krieg, H. Smola, *J. Invest. Dermatol.* **2007**, 127, 998.
- [190] E. Schrödinger, *What Is Life? The Physical Aspect of the Living Cell*, University Press, Cambridge, England **1944**.
- [191] F. Lipmann, *Adv. Enzymol.* **1941**, 1, 99.
- [192] A. G. Camus, *Histoire des Animaux d'Aristote*, Veuve DeSaint, Paris, France **1783**, p. 4.
- [193] A. Trembley, *Mémoires Pour Servir à l'Histoire d'un genre de Polyypes d'eau Douce à Bras en Forme de Cornes*, Chez Jean & Herman Verbeek, Leiden, Netherlands **1744**.
- [194] T. H. Morgan, *Regeneration*, Macmillan and Co., London, England **1901**.
- [195] P. M. Gilbert, K. L. Havenstrite, K. E. Magnusson, A. Sacco, N. A. Leonardi, P. Kraft, N. K. Nguyen, S. Thrun, M. P. Lutolf, H. M. Blau, *Science* **2010**, 329, 1078.
- [196] S. H. Tan, Y. Swathi, S. Tan, J. Goh, R. Seishima, K. Murakami, M. Oshima, T. Tsuji, P. Phuah, L. T. Tan, E. Wong, A. Fatehullah, T. Sheng, S. W. T. Ho, H. I. Grabsch, S. Srivastava, M. Teh, S. L. I. J. Denil, S. Mustafah, P. Tan, A. Shabbir, J. So, K. G. Yeoh, N. Barker, *Nature* **2020**, 578, 437.
- [197] P. Abreu, *Biomed. Pharmacother.* **2018**, 103, 463.
- [198] X. Li, *Acta Biochim. Biophys. Sin. (Shanghai)* **2013**, 45, 51.
- [199] A. H. Tang, T. A. Rando, *EMBO J.* **2014**, 33, 2782.
- [200] Y. Zhang, P. Cui, Y. Li, G. Feng, M. Tong, L. Guo, T. Li, L. Liu, W. Li, Q. Zhou, *FASEB J.* **2018**, 32, 1891.
- [201] J. K. Mouw, G. Ou, V. M. Weaver, *Nat. Rev. Mol. Cell Biol.* **2014**, 15, 771.
- [202] E. Krieg, M. M. Bastings, P. Besenius, B. Rybtchinski, *Chem. Rev.* **2016**, 116, 2414.
- [203] L. B. Gower, *Chem. Rev.* **2008**, 108, 4551.
- [204] M. K. Rasmussen, J. N. Pedersen, R. Marie, *Nat. Commun.* **2020**, 11, 2337.



Werner E.G. Müller is a pioneer professor in the field of enzyme-based biomineralization and bioinspired/biomimetic nanoparticles for applications in regenerative medicine. His scientific achievements, including molecular evolution and antiviral/anticancer agents, as well as biomaterials development, have been recognized with an ERC Advanced Investigator Grant and three ERC Proof-of-Concept Grants. More recently, his research focus has been on energy-delivering biomaterials/particles based on physiological inorganic polyphosphate, especially for wound and bone/cartilage repair. He was/is the coordinator of EU, BMBF, and BMWi projects and has received more than 20 worldwide awards. Author of more than 1200 publications; H-index 107 (Google Scholar).



Meik Neufurth earned his Ph.D. in Biology from Johannes Gutenberg University Mainz in 2011. After a postdoctoral position at the Institute for Zoology of Mainz University, he joined the group of W.E.G. Müller in 2012 at the University Medical Center. In between, he worked as a researcher in an EU-Marie Curie project at NanotecMARIN GmbH, Mainz. He has been leading the 3D printing laboratory of the University group since 2014. His current research topics are regeneratively active biomaterials, including GMP-certified polyphosphate, 3D-bioprinting/molding of tissue-like implants for bones and teeth, and materials for wound healing. Author/co-author of 60 peer-reviewed publications.



Shunfeng Wang finished his master's degree thesis under the supervision of W.E.G. Müller at the Institute for Physiological Chemistry, University Medical Center Mainz. Based on his good achievements, he continued with his doctoral degree study again under the supervision of Prof. Müller and finished his Ph.D. in 2018. During these studies, he was involved in a Marie Curie Secondment project at the Ruđer Bošković Institute, Croatia. At present, the focus of his research work is on the development of morphogenetically active inorganic materials such as biosilica and polyphosphate for bone regeneration and wound healing.



Heinz C. Schröder received his doctorate in chemistry and medicine with the highest distinction. After his postdoc period at Mainz University and the MPI for Biophysical Chemistry, Göttingen, funded by a Liebig scholarship (1982–1984) and at the National Cancer Center, Tokyo, he has been a professor at the University Medical Center since 1985. Among his main achievements are the discovery of several enzymes involved in polyadenylate and 2–5A metabolism. His current interest is the mode of action of biogenic nanoparticles. He has received several awards and authored/coauthored ≈ 600 publications. Together with W.E.G. Müller, he was a coordinator/partner in 20 EU-projects.



Xiaohong Wang is a materials scientist who became a professor in inorganic chemistry in 2005. She has extensive experience in the development and elucidation of the biological effects of bio-nanoparticles/materials for tissue regeneration, also including an understanding of the underlying molecular mechanisms. Since 2006 she has been working together with W.E.G. Müller's group and subsequently joined his group in 2010. The main focus of her research lies in the enzymatic formation of calcium carbonate bio-seeds in bone mineralization and the mechanism of biogenetically formed silica. Her scientific work was supported by several grants (as PI), including EU and BMBF projects. More than 300 publications (H-index 42; WoS).